A Model for H2O Solubility Mechanisms in Albite Melts from Infrared Spectroscopy and Molecular-Orbital Calculations

Article *in* Geochimica et Cosmochimica Acta · March 1993

DOI: 10.1016/0016-7037(93)90039-Y

2 authors, including:

J. D. Kubicki
University of Texas at El Paso
258 PUBLICATIONS **7,827** CITATIONS

SEE PROFILE

Geochimica et Cosmochimica Acta Vol. 57, pp. 1039–1052

0016-7037/93/$6.00 + .00

A model for H_2O solubility mechanisms in albite melts from infrared spectroscopy and molecular orbital calculations

DAN SYKES and J. D. KUBICKI
Division of Geological and Planetary Sciences, 170-25, California Institute of Technology, Pasadena, CA 91125, USA

(*Received April* 3, 1992; *accepted in revised form August* 13, 1992)

Abstract—Infrared spectra of H_2O- and D_2O-$NaAlSi_3O_8$ (albite) glasses were measured and contain two major differences from the anhydrous glass spectra. The first is the presence of a number of bands above 3000 cm^{-1} arising from O-H stretching modes. The second change in hydrous glass spectra is the appearance of a shoulder at approximately 900 cm^{-1}. No frequency shift of the 900 cm^{-1} shoulder was detected with H-D substitution. We conclude, based on our infrared spectra and molecular orbital calculations as well as previous NMR (KOHN et al., 1989) and Raman (MYSEN and VIRGO, 1986a) spectra, that the 900 cm^{-1} band in the vibrational spectra of H_2O-albite glass arises from an Al-(OH) stretching vibration in an Al Q^3 site.

The model proposed in this paper is that below 30 mol% $[H_2O]_{tot}$, molecular water interacts with the network Al^{3+} to produce Al-(OH) and a minor concentration of Si-(OH) bonds. Above 30 mol% $[H_2O]_{tot}$, the dominant species is molecular H_2O, and H^+ exchanges with Na^+ at the charge-balancing site to produce molecular NaOH or hydrated $Na^+(H_2O)_n$ complexes in the melt.

INTRODUCTION

EXPLANATIONS OF WATER SOLUBILITY mechanisms in H_2O-SiO_2 melts commonly invoke the interaction of dissolved H_2O with bridging oxygens, resulting in the disruption of the extended network structure (STOLEN and WALRAFEN, 1976; MCMILLAN and REMMELE, 1986; MYSEN and VIRGO, 1986a). One reason for this is the strong decrease in viscosity of fully polymerized melts with addition of H_2O (DINGWELL and MYSEN, 1985; DINGWELL, 1987). Furthermore, a peak at 970 cm^{-1} in the Raman and infrared spectra and a peak near −100 ppm in the ^{29}Si NMR spectra of hydrous SiO_2 glasses appear and are ascribed to Si-(OH) bonds (MYSEN and VIRGO, 1986a; FARNAN et al., 1987). Isotopic substitution of D_2O for H_2O shifts the Raman peak maximum to 950 cm^{-1}, leading to the assignment of the 970 cm^{-1} peak to an Si-(OH) stretching mode (MYSEN and VIRGO, 1986a).

In fully polymerized aluminosilicate glasses, such as $NaAlSi_3O_8$, dissolved water results in the appearance of a peak near 900 cm^{-1} in the Raman and infrared spectra (MYSEN et al., 1980; MCMILLAN et al., 1983; MYSEN and VIRGO, 1986b; SILVER and STOLPER, 1989). Assignment of this peak to a specific structural feature is not as straightforward as in the H_2O-SiO_2 system. FREUND (1982) and MCMILLAN et al. (1983) proposed that the 900 cm^{-1} band could result from a mixture of Al-O-H stretching and bending modes analogous to that found in H_2O-SiO_2. MYSEN and VIRGO (1986b) argued against this because of the lack of a detectable H-D isotopic shift of the 900 cm^{-1} shoulder. Instead, they proposed the formation of NaOH and $Al(OH)_3$ "complexes" along with Si Q^2 sites as the water solubility mechanism.

KOHN et al. (1989) measured NMR spectra of hydrous albite glass and concluded that H_2O does not interact with the network cations (i.e., Al^{3+} and Si^{4+}). KOHN et al. (1989) argued against the MYSEN and VIRGO (1986b) model because there is no evidence in the MAS NMR spectra for a coordination change in Al^{3+} or for the formation of Si Q^2 sites as predicted by MYSEN and VIRGO (1986b). Instead, KOHN et al. (1989) propose exchange of H^+ and Na^+ throughout the entire solubility range of water in these melts with concomitant formation of NaOH and H-O_{br} bonds where O_{br} remains bonded to two tetrahedral cations (KOHN et al., 1992). Recent NMR spectra have shown that water does depolymerize silicate melts (MERWIN et al., 1991; KUMMERLEN et al., 1992) and that volatile species such as F^- interact preferentially with Al^{3+} over Si^{4+} and Na^+ (SCHALLER et al., 1992). MERWIN et al. (1991) concluded that the NMR spectra of KOHN et al. (1989) should be re-interpreted based on their NMR spectra of H_2O-$Na_2Si_4O_9$ glasses.

In order to resolve this controversy, we have collected transmission infrared spectra of hydrated (40 mol% H_2O) and deuterated (40 mol% D_2O) albite glasses. To support our interpretations of the hydrous glass spectra and evaluate previous models, we have performed molecular orbital (MO) calculations on NaOH, $[Na(H_2O)_n]^+$, $Al(OH)_3$, $[Al(OH)_4]^-$, $[Al(OH)_3ONa]^-$, $Si(OH)_4$, H_7SiAlO_7, and $(H_6Si_mAl_nO_7)^{n-}$ (where $m + n = 2$) molecules and their deuterium analogs. The MO calculations provide Raman and infrared frequencies of the vibrational modes for these molecules which may then be related to changes in the vibrational (MORTIER et al., 1984; MURAKAMI and SAKKA, 1987; LASAGA and GIBBS, 1988; HILL and SAUER, 1989) and NMR spectra (WOLFF et al., 1986, 1989) of silicates. Similar molecular models have been used previously to understand important aspects of reactions in silicate glasses (UCHINO et al., 1991). We combine these new experimental and theoretical results with the previously measured Raman (MYSEN and VIRGO, 1986b) and NMR spectra (KOHN et al., 1989) as well as with viscosity (DINGWELL, 1987) and H_2O speciation (STOLPER, 1982; SILVER and STOLPER, 1989; ZHANG et al., 1991; SILVER et al., 1990) studies to formulate a model that is consistent with a wide range of data on the system H_2O-$NaAlSi_3O_8$.

METHODS

Experimental

Samples were synthesized at 2 GPa as follows. A predetermined amount of D_2O or triple-distilled H_2O was loaded into the base of an open-ended 3.8 mm OD Pt-capsule with a microsyringe. Sixty-five milligrams of glass powder were then loaded into the capsule and the entire assembly weighed. The capsule was then crimped, placed in a water bath, and triple welded.

The 2 GPa runs (1550°C) were performed in a 19.0 mm solid-media piston-cylinder apparatus (BOYD and ENGLAND, 1960) using a CaF_2 furnace assembly. The 'hot piston-out' technique was used. Temperature was monitored with a W5Re-W26Re thermocouple with no pressure correction on the emf output. Run durations of 5 min and 3 h were used to determine if H_2O-D_2O exchange occurred through the capsule. The runs were terminated by disconnecting power to the furnace with a quench rate of $\approx$200 to 500°C/s.

Transmission FTIR spectra (1800–400 cm^{-1}) of powdered samples contained in KBr pellets (1 mg sample: 200 mg KBr) were obtained with a Nicolet 60SX spectrometer fitted with a ceramic Globar source, Michelson interferometer, KBr beamsplitter, and an HgCdTe detector. Transmission FTIR spectra (7000–1850 cm^{-1}) of polished glass plates were obtained with the Nicolet 60SX spectrometer with a W-filament source, CaF_2 beamsplitter, and InSb detector. Spectra were compiled from 2048 scans.

Theoretical

Hartree-Fock, molecular orbital calculations were performed with GAUSSIAN 90 (FRISCH et al., 1990) on an Alliant FX-80 computer (Beckman Institute) and Cray Y-MP (Pittsburgh Supercomputing Center). 3-21G* basis sets were employed for each molecule (G = Gaussian functions used to approximate atomic orbitals, 3-21 = 3 Gaussians per atomic orbital with the valence electrons represented with double-zeta Gaussians, and * indicates that *d*-orbitals were used for second row atoms as polarization functions). This basis set predicts molecular geometries and frequencies fairly well in zeolites (SAUER, 1989). Larger basis sets may provide more accurate molecular structures and vibrational frequencies; however, comparison of our predicted spectra for H_4SiO_4 and $H_6Si_2O_7$ with higher level calculations (i.e., 6-31G*; LASAGA and GIBBS, 1991) shows that vibrational modes and frequencies are similar in both sets of calculations. The neglect of electron correlation in these calculations (ANDZELM and WIMMER, 1991) increases the predicted vibrational frequencies by approximately 10% over the same modes measured in solid silicates (HESS et al., 1986). Hence, all reported frequencies are corrected by 10% from the actual MO values for ease of comparison between theoretical and experimental vibrational modes. This is a common procedure used in molecular modelling of condensed phases (MORTIER et al., 1984). Although the actual MO frequencies may be 10% higher than actually observed, the changes in frequency of a mode with isotopic substitution are more accurate when compared to experiment (KUBICKI and SYKES, 1993a). For example, the Si-(OH) vibrational modes in $H_6Si_2O_7$ have isotopic shifts of 20–40 cm^{-1} (see Appendix A), consistent with the measured 20 cm^{-1} isotopic shift with deuteration of the Si-(OH) vibration in hydrous silica glass. Also, the MO-predicted $^{16}O \rightarrow {}^{18}O$ frequency shift of the bridging oxygen breathing mode in rings of three SiO_4 tetrahedra (KUBICKI and SYKES, 1993a) are close to the measured shift of these rings in SiO_2 glass (GALEENER and MIKKELSON, 1982).

H_4SiO_4 and $[H_4AlO_4]^{1-}$ were calculated with S_4 symmetry and $Al(OH)_3$ with C_{3v} symmetry. All other molecules were allowed to optimize without any symmetry constraints. For example, in $H_6Si_2O_7$, all Si-O_{br}, Si-O_{nbr}, and O-H distances were allowed to vary independently, as well as all bond angles and dihedral angles within the molecule, for a total of 39 (i.e., $3N - 6$, where N = the number of atoms) independent parameters. Structural parameters were then varied according to the Berny optimization scheme (FRISCH et al., 1990) in order to determine a minimum in the potential energy surface of the molecule. At a minimum energy structure, the Hessian matrix (i.e., $\partial^2 V/\partial q_i \partial q_j$ of all atoms, where V is the potential energy and q is a spatial coordinate) is weighted by the reduced mass of atoms i and j to give a vibrational matrix (LASAGA and GIBBS, 1988). Diagonalization of the vibrational matrix results in eigenvalues proportional to the square of the vibrational frequency (i.e., $\lambda_k = (2\pi\nu_k)^2$, where ν_k is the vibrational frequency) and eigenvectors of the vibrational modes. The program calculates the electronic structure of the molecule as a function of nuclear coordinates; hence, the dipolar and polarizability derivatives may be calculated for each mode giving the infrared and Raman intensities of the frequency. Isotopic shifts are calculated by resolving the Hessian for the molecule in the optimized geometry with isotopic substitutions on any given site.

RESULTS

Experimental

Infrared spectra of the powdered samples are shown in Fig. 1. The spectrum of anhydrous albite glass is similar to the infrared spectra of a previous investigation (SILVER and STOLPER, 1989). In the hydrous and deuterated samples, a shoulder has developed near 900 cm^{-1} on the high-frequency envelope. H_2O- and D_2O-albite glass spectra were normalized to the main low-frequency peak in the H_2O-albite glass, and then subtracted to discern the existence of any isotopic shift. No measurable shifts were found, however. The intensity of the shoulder relative to the intensity of the main low-frequency peak near 440 cm^{-1} decreases with deuteration. The ratio of the shoulder to the 440 cm^{-1} peak is 0.60 in the H_2O-bearing glass and 0.54 in the D_2O-bearing glass. A similar effect has been measured in the Raman spectra of H_2O-D_2O glasses by MCMILLAN et al. (1993).

The actual frequency of this vibrational mode is difficult to resolve given the relatively broad width of the high frequency envelope. However, this vibrational mode is better

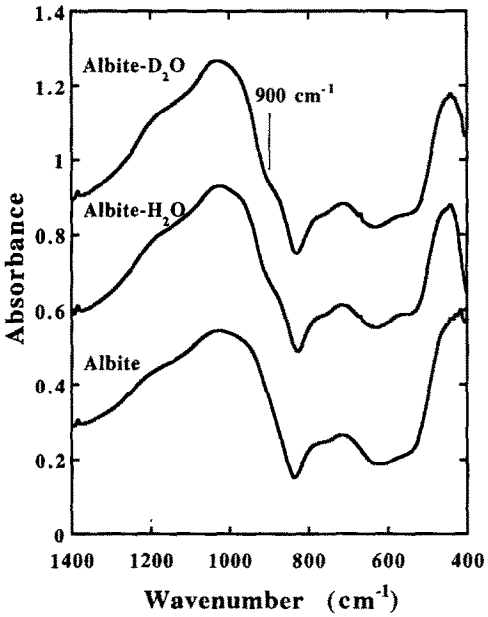

FIG. 1. Infrared spectra of albite, hydrous albite, and deuterated albite glasses shown above are from powdered glasses in KBr pellets. The main difference between the hydrous and anhydrous glasses is the shoulder at 900 cm^{-1} in the hydrous glass. A peak shift was not detected with substitution of D_2O for H_2O in the sample, but the intensity of the 900 cm^{-1} shoulder is diminished in the D_2O-albite glass spectrum. Constants of 0.3 and 0.6 absorbance units were added to the H_2O and D_2O spectra, respectively, for clarity.

resolved in the Raman spectra of hydrous albite glasses and appears as a peak with a maximum at 900 cm^{-1} (MYSEN and VIRGO, 1986b; MCMILLAN et al., 1993). For clarity and consistency with previous investigations, the frequency of this vibrational mode will be referred to as 900 cm^{-1} although the inflection point in the present spectra may be closer to 880 cm^{-1}.

Infrared spectra of the polished plates are shown in Fig. 2. The most intense peak at 3530 cm^{-1} and the peak at 4000 cm^{-1} in hydrous albite result from fundamental O-H stretching modes independent of water speciation (STOLPER, 1982; NEWMAN et al., 1986; SILVER and STOLPER, 1989). Combination *X*-O-H stretching modes (where *X* is a cation) may contribute to the intensity of the 4500 cm^{-1} peak (SILVER and STOLPER, 1989). The peak at 5200 cm^{-1} arises from a mixed bending-stretching mode of molecular water. All the above vibrations are also apparent in the D_2O-albite sample with the most intense peak shifted to 2570 cm^{-1}. The observed frequency shift from 3530 to 2570 cm^{-1} with deuteration corresponds to the predicted isotopic frequency shift of a simple harmonic oscillator indicating that the vibration is an internal O-H mode.

Total water contents were calculated from the molar absorption coefficients for hydrous albite glass of SILVER and STOLPER (1989) with a density of 2410 g/L. The total amount of H_2O calculated ($[H_2O]_{tot}$ = 5.02 wt%, $[OH^-]$ = 1.92 wt%, $[H_2O]_{mol}$ = 3.10 wt%) compares well with the amount assumed to be added to the capsule (5.0 wt%). The amount of $[H_2O]_{tot}$ calculated for the D_2O-albite sample is approximately a factor of 750 times higher than the purity of the starting D_2O (i.e., H_2O/D_2O in albite glass, 0.65/4.35 = 0.15 vs. H_2O/D_2O in the heavy water, 0.02/99.98 = 0.0002). The higher H_2O concentration results from hydrogen diffusion through the Pt-capsule during sample synthesis. A sample synthesized at pressure and temperature for 3 h had peaks of approximately equal intensity at 3530 cm^{-1} and 2570 cm^{-1} indicating a significant amount of hydrogen diffusion into the sample and elevated concentrations of H_2O. Hence, it is imperative that synthesis times are kept to a minimum in order to minimize H-D exchange through the capsule.

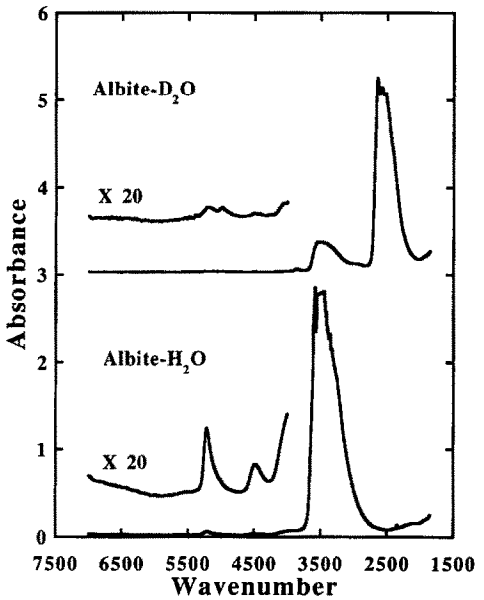

FIG. 2. Infrared spectra of H_2O- and D_2O-albite glasses (≈5 wt% H_2O or D_2O) from polished plates (≈75 μm thick). Frequency shifts due to isotopic substitution of D for H are consistent with the values expected from a harmonic oscillator model for an O-H stretch and from the molecular orbital calculations of this study.

Theoretical

Optimized structures and energies of each molecule are listed in Table 1. Graphic representations of the equilibrium molecular structures for the $[H_6Si_mAl_nO_7]^{n-}$ dimers are plotted in Fig. 3. The first observation that can be made from the results is that MO theory predicts that the Al-avoidance principle (LOWENSTEIN, 1954) should be obeyed. The theoretical reaction

$$¼[H_6Si_2O_7] + ¼[H_6Al_2O_7]^{2-} \Leftrightarrow ½[H_6SiAlO_7]^{1-}$$

favors the Si-Al dimer by approximately −150 kJ/mol. This is much larger than the observed enthalpy of mixing in aluminosilicate glasses (i.e., −22.6 kJ/mol; NAVROTSKY et al., 1982), but the qualitative behavior of the isolated molecules and condensed phases are similar. (See NAVROTSKY et al., 1985, for a discussion of the reasons why the above theoretical reaction overestimates the enthalpy of this reaction in glasses.) In addition, *T*-O bonds, and *T*-O-*T* and O-*T*-O angles in the clusters, are similar to those measured in silicate crystals and glasses. For example, MOZZI and WARREN (1969) predict an average Si-O-Si angle of 144° in SiO_2 glass from X-ray scattering experiments; whereas these calculations predict an equilibrium Si-O-Si angle of 141.5° in $H_6Si_2O_7$ (see GIBBS, 1982, for a more complete discussion of these relationships).

In general, the correspondence is good between the vibrational modes calculated in each frequency range and those interpreted from experimental spectra (Fig. 4). Hence, we consider the theoretical frequencies as analogs for vibrations in glasses. As mentioned previously, theoretical frequencies discussed in the text have been corrected by 10% to facilitate discussion and comparison with the experimental results. Uncorrected values for all molecules are listed in Appendix A.

The theoretical spectra of the dimers may be divided into five regions that correspond to the experimental assignments of vibrational modes in silicates. Below 450 cm^{-1}, O-Si-O bending modes dominate the theoretical spectra (e.g., Fig. 5a) as suggested by MOENKE (1974) for glass spectra. Between 400 and 850 cm^{-1}, *T*-O-*T* angle bending and bridging oxygen stretching modes are predominant (e.g., Fig. 5b) in our calculations. Many investigators (FURUKAWA et al., 1981; MATSON et al., 1983; MCMILLAN, 1989) have associated bands in this frequency range of silicate glass spectra to this type of vibrational mode. *T*-O_{nbr} stretching modes are predicted in the range of 800 to 1000 cm^{-1} (e.g., Fig. 5c) as is observed in a wide variety of silicates (MCMILLAN, 1989). Furthermore, a set of *T*-O_{br} stretches have vibrational frequencies from 1000 to 1200 cm^{-1} (Fig. 5d). This is consistent with the relative frequencies of Si-O_{br} vs. Si-(OH) stretches in hydrous SiO_2 glass (STOLEN and WALRAFEN, 1976). Above 1350 cm^{-1}, the theoretical vibrations consist entirely of O-H bends and stretches.

Table 1 - Ab initio structures and energies of hydrous aluminosilicate molecular groups at the 3-21G* level. "⟨ ⟩" indicate average values.

Molecule	Energy (10^6 kJ/mol)	T-O (Å)	O-H (Å)	T-O-T (Degrees)	O-T-O (Degrees)	T-O-H (Degrees)
H_4SiO_4	1.5434	1.6484	0.9616		106.00[f] 116.66[g]	114.54
$[H_4AlO_4]^{1-}$	1.4205	1.7509	0.9660		107.12[f] 114.27[g]	114.39
$H_6Si_2O_7$	2.8884	<1.62>[a] <1.62>[b]	<0.96> 0.959[f] 0.969[g]	141.53	<109.48> 105.87[f] 114.17[g]	<124.32> 119.32[f] 126.50[g]
$[H_6SiAlO_7]^{1-}$	2.7656	<1.64>[a] 1.60[b] <1.75>[c] 1.75[d]	<0.97>[a] <0.96>[c]	131.79	<109.48>[a] <109.45>[c]	<115.41>[a] <118.73>[c]
$[H_6Al_2O_7]^{2-}$	2.6422	<1.77>[c] <1.72>[d]	<0.97> 0.969[f] 0.971[g]	129.29	<109.41> 104.83[f] 114.00[g]	<108.23> 106.39[f] 110.99[g]
H_7SiAlO_7	2.7670	<1.60>[a] 1.67[b] <1.71>[c] 1.87[d]	<0.97> 0.955[f] 1.004[g]	128.68	<109.08> 92.91[f] 119.57[g]	<127.27> 118.82[f] 133.53[g]
Na(OH)	0.6193	1.8564[e]	0.9632			180.00[e]
$Al(OH)_3$	1.2233	1.6687	0.9547		120.0	135.52

a - Non-bridging oxygen bonded to Si.
b - Bridging oxygen bonded to Si.
c - Non-bridging oxygen bonded to Al.
d - Bridging oxygen bonded to Al.
e - Sodium-oxygen bond.
f - Minimum value.
g - Maximum value.

$Al(OH)_3$ was optimized to a trigonal planar geometry in these calculations although it was not constrained to this arrangement a priori. Al-(OH) stretching modes in $Al(OH)_3$ occur at 720 (Raman-active) and 970 cm^{-1} (IR-active). The 720 cm^{-1} vibration is the strongest Raman band below 4000 cm^{-1} in the theoretical spectrum of this molecule. This is similar to the frequency of the Al-(OH) bands in $[H_4AlO_4]^{1-}$ and $[H_6Al_2O_7]^{2-}$ where the Al-(OH) stretches range from 600 to 1100 cm^{-1}. Calculated Mulliken charges and electric field gradients (EFG's) at the Al nucleus in $Al(OH)_3$ and $[Al(OH)_4]^-$ clusters are given in Table 2. The correlation of Mulliken charges with NMR chemical shifts has been documented by WOLFF et al. (1986, 1989). In quadrupolar nuclei, such as ^{27}Al and ^{23}Na, the EFG about the nucleus interacts with the nuclear quadrupole moment and affects the NMR peak position and lineshape (BLINC, 1976; ENGELHARDT and MICHEL, 1987). MO theory predicts significant differences in the EFG between Al in 3- vs. 4-fold coordination consistent with measured ^{27}Al NMR parameters in organometallic compounds (BEN et al., 1991). A significant change in the ^{27}Al MAS NMR spectra of albite glass should occur upon hydration if $Al(OH)_3$ forms.

MO calculations were also performed on Na^+ with four point charges (similar to a charge-balancing site in a glass), Na(OH), $[Na(H_2O)]^+$, and $[Na(H_2O)_6]^+$. Na(OH) has an infrared-active mode at 370 cm^{-1} (an O-H stretch with Na-O-H bend) and a Raman-active mode at 635 cm^{-1} (an Na-(OH) stretching mode). The Mulliken charges and EFG's for these clusters are listed in Table 2. Na^+ is polarized in Na(OH) and $[Na(H_2O)_n]^+$ in contrast to the spherical electron cloud distribution when Na^+ is in a charge-balancing site. Hence, the higher EFG at Na^+ would change the C_q of ^{27}Na in MAS NMR spectra significantly with formation of either Na(OH) or $[Na(H_2O)_n]^+$ from Na^+ in a charge-balancing site.

Theoretical isotopic shifts for the $[H_6SiAlO_7]^{1-}$ molecule are listed in Table 3. Since the only significant differences between anhydrous and hydrous vibrational spectra of albite glass occur at approximately 900 cm^{-1} and above 3000 cm^{-1}, we will focus on these regions of the theoretical spectra.

The MO-predicted O-H stretching frequency shifts are nearly identical to those predicted by harmonic theory (WILSON et al., 1955) with substitution of D for H. In Appendix A, the ratios of simple O-H to O-D stretches above 2500

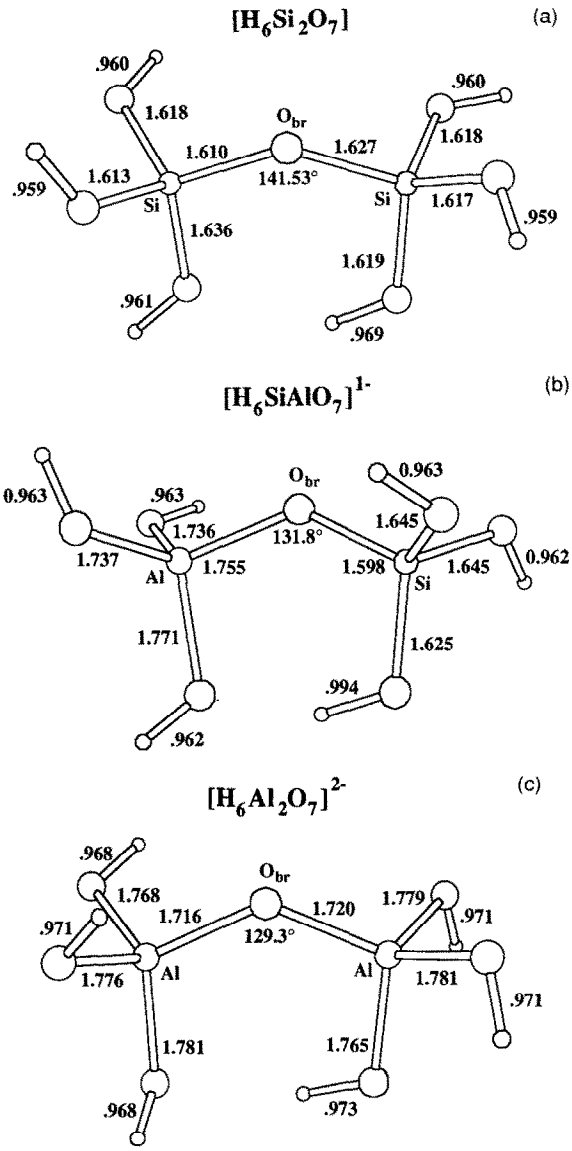

FIG. 3. Computer-generated graphics (from the program ATOMS; DOWTY, 1990) of the stationary points at the 3-21G* level of the molecules $H_6Si_2O_7$ (a), $[H_6SiAlO_7]^{1-}$ (b), and $[H_6Al_2O_7]^{2-}$ (c) are plotted above. These structures are similar to the results of GEISINGER et al. (1985) at the STO-3G level for $H_6Si_2O_7$ and $[H_6SiAlO_7]^{1-}$; but the Al-dimer has a much smaller intertetrahedral angle in this study (129.3 vs. 151°) which is more consistent with experimental data on intertetrahedral angles in aluminosilicates (GEISINGER et al., 1985).

cm^{-1} range from 1.370 to 1.374. These predictions are close to the isotopic frequency shifts measured in hydrous albite glass (Fig. 2; MYSEN and VIRGO, 1986b). Thus, the theoretical isotopic frequency shifts calculated for these molecules can be used as reasonable analogs for the shifts in aluminosilicate glasses.

Tetrahedral cation substitutions have a significant effect on the O-H stretching frequencies predicted for the dimers. The average O-H stretch of hydroxyl groups bonded to Al are approximately 140 cm^{-1} lower than in their (Si)O-H counterparts. This is consistent with the observed decrease in frequency of the peak near 4500 cm^{-1} as the (Al/Al + Si) ratio of hydrous glasses increases (STONE and WALRAFEN, 1982; NEWMAN et al., 1986; MYSEN and VIRGO, 1986b; SILVER and STOLPER, 1989). In addition to the compositional shifts, there is a significant difference in the frequencies of the O-H stretches between the isolated tetrahedra and the dimers. In H_4SiO_4, the O-H stretches are near 3570 cm^{-1} with a range of 4 cm^{-1}. In the $H_6Si_2O_7$ molecule, O-H stretches range from 3470 to 3595 cm^{-1}. The average O-H stretch in Q^0 and Q^1 SiO_4 tetrahedra is nearly identical according to these calculations. However, the average O-H stretch in the dimer is lowered by one mode at 3470 cm^{-1} where an (OH)—(OH) bridge forms between tetrahedra (BURKHARD et al., 1991; KUBICKI and SYKES, 1993b). The other modes are from 5 to 25 cm^{-1} higher than the O-H stretches in H_4SiO_4. On the other hand, $(OH)^-$ groups bonded to Al^{3+} undergo a decrease in the average O-H

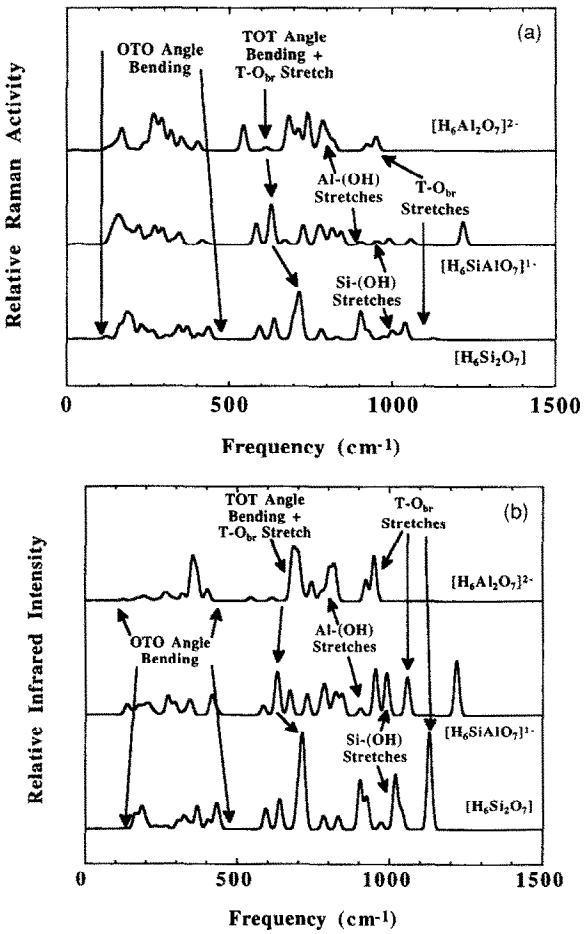

FIG. 4. Synthetic theoretical spectra (a—Raman; b—infrared) of the aluminosilicate dimers are plotted above to show the correspondence between vibrational modes and frequencies in the molecules and aluminosilicate glasses. The figure also graphically illustrates the types of shifts in modes expected with substitution of Al^{3+} for Si^{4+} in aluminosilicate glasses. Most importantly, the v_s mode decreases with substitution of Al^{3+} for Si^{4+} as is observed in melilite Raman spectra (SHARMA et al., 1988).

Table 2 - Atomic charges and electric field gradients (EFG) on aluminum and sodium are listed below as calculated from GAUSSIAN 90 at the 3-21G* level.

Molecule	Mulliken charge	EFG		
		X	Y	Z
Na^+ (4 pt. charges)	1.00	0.00	0.00	0.00
NaOH	0.53	-0.03	-0.03	0.05
$Na^+(H_2O)$	0.85	-0.07	-0.04	0.11
$Na^+(H_2O)_6$	0.26	-0.02	-0.01	0.02
$Al(OH)_3$	1.23	-0.52	0.26	0.26
$[Al(OH)_4]^{1-}$	0.97	-0.01	-0.01	0.02
$[NaAlO(OH)_3]^{1-}$	0.87 (Al)	-0.20	-0.04	0.23
	0.33 (Na)	-0.09	-0.03	0.12
$[H_6SiAlO_7]^{1-}$	1.03	-0.09	-0.03	0.12
$[H_7SiAlO_7]$	1.15	-0.36	0.14	0.22

stretching frequency with polymerization from $[Al(OH)_4]^{1-}$ to $[H_6Al_2O_7]^{2-}$. From these results, we predict that O-H stretching frequencies bonded to Si in glasses would increase in the order $Q^0 \rightarrow Q^1 \rightarrow Q^2 \rightarrow Q^3$. The opposite would be true for O-H stretches bonded to Al. These trends accurately predict the calculated O-H stretch frequencies in Al- and Si-Q^2 sites in theoretical 3-membered rings (KUBICKI and SYKES, 1993a). However, if the predicted range of vibrational

Table 3. Corrected frequencies of vibrational modes in the $[H_6SiAlO_7]^{1-}$ molecule. Vibrational modes are given in order of the dominant displacements that contribute to the mode. The reduced mass, theoretical isotopic shifts, and frequency ratios for each vibrational mode upon deuteration are also given.

Frequency	Motion	μ(H)	μ(D)	H-D Shift	[νH/νD]
30.9	OTO, TOH	7.3	7.9	1.2	1.039
42.9	OAlO, TOT, TOH	8.0	8.4	1.5	1.035
135.3	(Al)O-H, OAlO	2.2	2.9	23.5	1.210
147.8	(Al)O-H, OAlO, AlOH	1.9	2.5	29.7	1.252
161.4	(Al)O-H, OAlO, AlOH	1.6	2.5	35.5	1.282
175.1	(Si)O-H, OTO, TOH	1.4	2.2	44.1	1.337
192.2	(Si)O-H, OTO, TOH	2.1	2.7	31.4	1.195
207.5	(Si)O-H, OTO, TOH	2.7	6.7	21.2	1.114
223.9	(Al)O-H, OTO, TOH	2.3	5.2	21.1	1.104
250.1	O-H, OTO, TOH	2.6	4.8	25.0	1.111
271.1	O-H, OTO, TOH	1.6	5.3	44.4	1.196
291.5	OTO, (Si)O-H, TOH	2.2	4.5	35.6	1.139
297.5	TOT, OTO, (Al)O-H	5.1	6.8	16.3	1.058
324.8	OTO, (Al)O-H, TOH	3.0	4.8	31.9	1.109
340.7	OTO, (Al)O-H, TOH	5.4	4.6	26.4	1.084
348.8	OTO, (Si)O-H, TOH	3.6	11.4	17.6	1.053
416.3	OTO, TOH	7.2	6.7	19.1	1.048
432.6	OTO, TOT, TOH	6.9	8.2	17.8	1.043
584.6	$T\text{-}O_{br}$, TOT, Al-O-H	6.8	2.6	38.2	1.070
626.3	Al-(OH), (Al)O-H, AlOH	1.4	3.1	148.9	1.312
632.8	Al-(OH), (Al)O-H, AlOH	1.4	3.9	133.0	1.266
671.9	$Al\text{-}O_{br}$, TOT, Al-O-H	4.0	5.8	81.0	1.137
728.5	Al-(OH), (Al)O-H, TOH	1.6	2.6	111.1	1.180
774.2	Al-(OH), Si-O-H, TOH	3.5	3.8	137.0	1.215
787.1	Al-(OH), (Si)O-H, TOH	2.6	2.6	25.1	1.033
814.6	O-H, T-(OH), SiOH	2.0	9.6	119.5	1.172
825.6	Al-(OH), (Al)O-H, TOH	2.1	13.9	20.9	1.026
844.7	T-(OH), TOH, Si-O-H	4.0	11.0	30.1	1.037
904.0	Si-(OH), (Si)O-H, TOH	1.4	8.4	235.4	1.352
954.2	Si-(OH), Si-O-H, TOT	3.6	3.1	55.7	1.062
991.2	$T\text{-}O_{br}$, Si-(OH), OSiO	5.0	11.5	64.8	1.070
1057.9	$T\text{-}O_{br}$, Si-(OH), OTO	8.9	16.5	84.7	1.087
1218.3	(Si)O-H, SiOH, OSiO	1.1	15.5	153.4	1.144
3036.2	O-H	1.1	2.2	823.2	1.372
3516.1	O-H	1.1	2.2	955.2	1.373
3516.7	O-H	1.1	2.2	955.4	1.373
3540.2	O-H	1.1	2.2	961.8	1.373
3549.2	O-H	1.1	2.2	966.1	1.374
3553.3	O-H	1.1	2.2	967.2	1.374

frequencies is accurate, the FWHM may also increase with polymerization, and these spectral shifts may be difficult to detect. In addition, any H-bonding between the $(OH)^-$ group and other oxygens in the glass would significantly lower the O-H stretching frequency as evidenced by the O-H stretch at 3470 cm^{-1} that is H-bonded to another oxygen in the dimer.

Isotopic frequency shifts of vibrational modes in the 700 to 1000 cm^{-1} region are more complex than the O-H stretches. The modes are mixtures of different types of stretching and bending motions involving many of the atoms in the molecule at once (Fig. 4, 5; Appendix A). Frequency shifts of modes in this frequency range with deuteration can be small (e.g., 20 cm^{-1} for the 825 cm^{-1} Al-(OH) stretch in $[H_6SiAlO_7]^{1-}$) because the reduced mass of the mode is large compared to O-H stretching modes (Appendix A). Large isotopic frequency shifts are calculated only for modes involving an O-H stretch with a small reduced mass. There are numerous modes associated with T-(OH) in these theoretical molecules because there are six T-(OH) bonds. In the glass, there is only one broad band associated with stretching in one type of site. However, it is clear that Al-(OH) stretches are common throughout the frequency range from 700 to 1000 cm^{-1}; whereas, Si-(OH) stretches and T-O_{br} stretches occur between 900 to 1200 cm^{-1}. The average Si-(OH) stretch in $H_6Si_2O_7$ is $\approx$960 cm^{-1}. This frequency is close to the Si-(OH) stretch in hydrous silica glass (i.e., 970 cm^{-1}; MYSEN and VIRGO, 1986a). The Raman-active Al-(OH) stretch in $Al(OH)_3$ and Na-(OH) stretch are too low in frequency to give rise to the 900 cm^{-1} shoulder in hydrous albite. Thus, Al-(OH) stretches in network-forming (i.e., tetrahedral) Al^{3+} cations seem to be the best assignment for the 900 cm^{-1} shoulder.

In modes dominated by T-O_{br} stretches, the average Si-O_{br} stretch in $H_6Si_2O_7$ is $\approx$1000 cm^{-1}; whereas, in $[H_6SiAlO_7]^{1-}$, this mode averages a frequency of $\approx$1025 cm^{-1}. This is caused by the shorter Si-O_{br} bond distance in $[H_6SiAlO_7]^{1-}$ (1.60 Å) vs. $H_6Si_2O_7$ (1.62 Å). In $[H_6Al_2O_7]^{2-}$, the average Al-O_{br} stretch is near 900 cm^{-1}. In $[H_6SiAlO_7]^{1-}$, this average is $\approx$830 cm^{-1} as the Al-O_{br} distance increases from 1.72 Å in $[H_6Al_2O_7]^{2-}$ to 1.75 Å. These shifts are for molecules without charge-balancing ions to compensate for the excess charge on the molecule, which may have an effect on the calculated frequencies. The effect of Na^+ charge-balancing ions on T-O_{br} frequencies is likely to lower T-O_{br} frequencies because GEISINGER et al. (1985) have shown that Na^+ lengthens T-O_{br} bonds when bonded to the bridging oxygen. However, it is likely that Na^+ ions in charge-balancing sites will have a smaller effect on the frequencies of T-O_{br} vibrations than the fully-bonded Na^+ ions of the GEISINGER et al. (1985) calculations.

Polymerization of the tetrahedral cations from Q^0 to Q^1 also has an effect on the T-(OH) stretching frequencies. In H_4SiO_4, the Si-(OH) stretches range from 700 to 1000 cm^{-1}, but in $H_6Si_2O_7$, these frequencies increase and range from 800 to 1040 cm^{-1} with a decrease in the Si-O_{nbr} bond distance from 1.65 to 1.62 Å. For aluminum, the polymerization effect is not significant as the Al-(OH) stretches are at 620 to 815 cm^{-1} in $[H_4AlO_4]^{1-}$ and at 615 to 820 cm^{-1} in $[H_6Al_2O_7]^{2-}$. This increase in Si-O stretching frequency with polymerization is consistent with measured Raman spectra (MCMILLAN, 1984). Furthermore, the expected changes from the theoretical Q^1 species ($[H_6SiAlO_7]^{1-}$) to the Q^3 species actually involved in the glass vibration could raise these calculated vibrational frequencies closer to the observed value of 900 cm^{-1}. Because we have not found a simple relationship

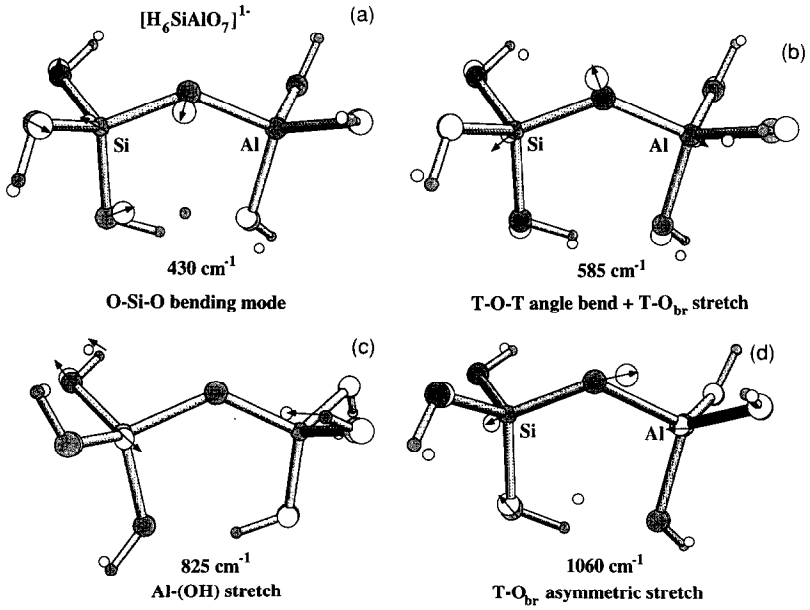

FIG. 5. Computer-generated graphics (ATOMS; DOWTY, 1990) of representative vibrational modes for each frequency region in the theoretical spectrum of $[H_6SiAlO_7]^{1-}$. The arrows illustrate displacements associated with the vibrational mode. (a) The dominant motion is from O-T-O angle bending at a frequency of 430 cm^{-1}; (b) the 585 cm^{-1} vibrational mode of T-O-T angle bending and T-O_{br} stretching; (c) an Al-(OH) stretching mode at 825 cm^{-1}; (d) a dominantly asymmetric T-O_{br} stretch at 1060 cm^{-1}.

between Q-speciation and the frequency of the T-(OH) vibrational mode, we cannot accurately predict the frequency of a T Q^3-(OH) stretch. MO calculations on Si and Al Q^3 species may be necessary to address this problem directly.

DISCUSSION

Previous Models

There are several competing models for H_2O solubility in albite melts. MYSEN et al. (1980) and MYSEN and VIRGO (1986b) assigned the 900 cm^{-1} feature in the Raman spectrum to symmetric Si-O_{nbr} stretches in SiO_3^{2-} units (i.e., Si Q^2 sites) because no H-D isotopic shift was measured and because of inferred polymerization changes based on results from curve-fitting the high-frequency envelope. FREUND (1982) suggested that the apparent lack of an observable (H-D) isotopic shift in the 900 cm^{-1} Raman band is a result of a relatively small shift combined with the broad nature of the 900 cm^{-1} band and the silicate stretching bands in this region. MCMILLAN et al. (1983) then suggested that the shoulder arises from Q^3 Al-(OH) vibrations.

KOHN et al. (1989) have presented a model based on $H^+ \rightarrow Na^+$ exchange and the formation of NaOH and $[Na(H_2O)_n]^+$ "complexes" for H_2O dissolution in albite melt to explain the ^{29}Si, ^{27}Al, ^{23}Na, and ^1H NMR spectra. Recently, PICHAVANT et al. (1992) attempted to explain the phase relations of hydrous quartz-feldspar melts based on a model similar to KOHN et al. (1989). The main difference in the PICHAVANT et al. (1992) model is that the $H^+ \rightarrow Na^+$ exchange leads to a full H-O_{br} bond (i.e., bond order = 1) rather than H^+ in a charge-balancing site (i.e., bond order = ¼). Based on the available spectroscopic data, we will attempt to demonstrate that the 900 cm^{-1} feature arises from Al-(OH) stretching as suggested by FREUND (1982) and MCMILLAN et al. (1983).

Isotopic shift factors calculated with harmonic theory depend on an assumption of the reduced mass of the vibration. MYSEN et al. (1980) assumed the H-D frequency shift should be $\approx$1.37 for the 900 cm^{-1} band if it were the result of an O-H stretch. FREUND (1982) pointed out that if the feature arose from oscillations of the (OH^-) group against a semi-rigid framework the H-D shift would be $\approx$1.018. If the 900 cm^{-1} band results from a vibrational mode involving significant Al^{3+} motion or AlOH angle bending, then the expected isotopic shift would be much less significant. Hence, from harmonic theory and MO calculations a H-D isotopic frequency shift less than 20 cm^{-1} is reasonable for the 900 cm^{-1} shoulder. There is a 10 cm^{-1} uncertainty in the peak fits of the Raman spectra of MYSEN and VIRGO (1986b), so the question of whether or not a shift occurs is indeterminate from their treatment of the Raman spectra. In fact, examination of the Raman spectra of a hydrous glass with (Al/Al + Si) = 0.125 (MYSEN and VIRGO, 1986b) shows that the 900 cm^{-1} peak does appear to shift with deuteration; however, the curve-fitting procedure disguises this shift as other components in the fit shift by as much as 10 cm^{-1} (MYSEN and VIRGO, 1986b). MYSEN and VIRGO's (1986b) exclusion of an Al-(OH) stretch assignment for the 900 cm^{-1} feature is unwarranted based on their data.

MYSEN and VIRGO (1986b) assumed that NaOH would have no Raman signal due to the ionic nature of the Na-(OH) bond, but the results of the MO calculations presented in this study indicate that this molecule can give rise to Raman-active vibrations. In fact, the peak MYSEN and VIRGO (1986b) detect near 635 cm^{-1} in the Raman spectra of albite glass with >30 mol% H_2O may be due to the Na-(OH) stretching frequency predicted at 636 cm^{-1}.

The MYSEN and VIRGO (1986b) model is incompatible with the more recent NMR spectra. Single-pulse and cross-polarization (MAS) NMR experiments (KOHN et al., 1989) indicate that neither $^{[6]}Al$ nor $^{[5]}Al$ sites are present in hydrous aluminosilicate glasses. ^{29}Si NMR spectra of hydrous albite glasses (KOHN et al., 1989) have no peaks corresponding to the ^{29}Si chemical shift of −77 ppm for Si Q^2-(ONa) sites (DUPREE et al., 1984; MURDOCH et al., 1985). Hence, the models of MYSEN et al. (1980) and MYSEN and VIRGO (1986b) based on the formation of the above species cannot be valid.

The main problem with the models of KOHN et al. (1989, 1992) and PICHAVANT et al. (1992) is that they do not explain adequately the development of the 900 cm^{-1} peak in the vibrational spectra of H_2O-albite glass. These authors have suggested (KOHN et al., 1992; PICHAVANT et al., 1992) that the 900 cm^{-1} shoulder arises from a Si-(O_{br}H)-Al linkage (Fig. 6) but provide no evidence to support this assertion.

MO results on the H_7SiAlO_7 molecule (Table 1; Appendix A) indicate that there is a weak Raman and moderate infrared peak near 900 cm^{-1} due to Si-O_{br} stretching with an H-D isotopic frequency shift of $\approx$30 cm^{-1}. However, these same calculations indicate that the T-O_{br} + TOT bending mode, ν_s, is shifted significantly with H^+ addition to the bridging oxygen. An approximately 180 cm^{-1} shift in this mode is predicted from 585 to 765 cm^{-1} between $[H_6SiAlO_7]^{1-}$ and H_7SiAlO_7. No such change is observed for the low-frequency ν_s peak in hydrous albite glass spectra. Second, the H-O_{br} stretching vibration is calculated to have significant Raman or infrared intensity at 380, 585, 1020, 1040, and 1090 cm^{-1}. There is no evidence that any of these peaks exist in the

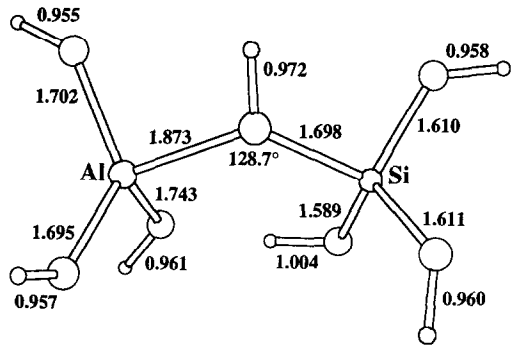

FIG. 6. A stable configuration of the H_7SiAlO_7 molecule at the 3-21G* level (ATOMS; DOWTY, 1990). The elongation of the Si-O_{br} and Al-O_{br} bonds connected with O_{br}-H causes a 300 cm^{-1} decrease in the Si-O_{br} and Al-O_{br} vibrational frequencies. However, the other T-O bonds in the molecule shorten and their vibrational frequencies increase. This effect is not observed in the experimental vibrational spectra of hydrous albite glasses.

vibrational spectra of hydrous albite glass. Third, the isotopic frequency shift of all H-O_{br} vibrations below 1200 cm^{-1} should be less than 20 cm^{-1} if the KOHN et al. (1992) model is correct. However, we have calculated the frequency shifts for the D-O_{br} bond in this molecule and find shifts of 6, 55, 90, 20, and 30 cm^{-1} for the above frequencies, respectively. The 1020 cm^{-1} vibration should be the strongest in the Raman spectra of hydrous albite if the Si-(O_{br}H)-Al species is present, so the 90 cm^{-1} shift associated with this peak would definitely be observed if it were present. Fourth, protonation of the Si-O-Al linkage significantly lengthens the Si-O bond according to our calculations (Table 1) and the models of KOHN et al. (1992) and PICHAVANT et al. (1992). The increase in the Si-O_{br} distance would lead to a more negative ^{29}Si chemical shift, which is not observed in the NMR spectra of hydrous albite glass (KOHN et al., 1989). Fifth, the EFG about Al increases significantly with protonation of the Si-O-Al linkage (Table 2), which would result in a concommitant increase in the quadrupole coupling constant and significant linebroadening. In contrast, the ^{27}Al linewidth decreases in the hydrous glasses.

KOHN et al. (1989) precluded the existence of Q^3 Al-(OH) sites because there is no peak near 70 ppm in the ^{27}Al MAS NMR spectra of hydrous albite glasses. This conclusion assumes that the ^{27}Al Q^3-(OH) chemical shift of a hydrous albite glass would be equivalent to the ^{27}Al Q^3-(OM) chemical shift of a crystalline layer silicate (KINSEY et al., 1985). However, their conclusion may be in error because the above assumption may not be valid. On the contrary, RYSKIN (1974) hypothesized that the nature of the *T*-O-H bond should be intermediate to that of *T*-O-*T* and *T*-O-*M* bonds (where *T* = Al or Si and *M* = alkali and alkaline earth cations). For example, the ^{29}Si MAS NMR resonance for Q^4 sites in SiO_2 glass is at −110 ppm (OESTRIKE et al., 1987) and for Q^3-(OM) sites in alkali disilicate glasses at −90 ppm, a 20 ppm shift (MURDOCH et al., 1985). Comparing these NMR shifts to Si-(OH) bonds, ^{29}Si MAS NMR resonance occurs at −100 ppm in Si Q^3-(OH) sites in hydrous SiO_2 glass (FARNAN et al., 1987) intermediate between the −110 ppm shift in Si-O-Si linkages and the −90 ppm shift in Si-O-*M* linkages. Hence, NMR spectroscopy indicates Si-(OH) linkages have intermediate character between Si-O-Si and Si-O-*M* linkages, so a large shift from 53 to 70 ppm may not be necessary in the ^{27}Al NMR spectra as Al Q^4 → Al Q^3-(OH).

KOHN et al. (1992) also preclude terminal Si-(OH) bonds (i.e., Si Q^3) because ^1H-^{29}Si cross-polarization NMR spectra show a wide distribution of H—Si distances with the mean H—Si distance larger than an Si-(OH) unit. On the other hand, these same authors propose Si-(O_{br}H)-Al linkages (Fig. 6) to explain the decrease in melt viscosity with addition of water and the 900 cm^{-1} feature in the vibrational spectra of the glass. Our calculations and those of GEISINGER et al. (1985), however, indicate a change in the Si-O_{br} bond distance of approximately 0.1 Å from $[H_6SiAlO_7]^{1-}$ to H_7SiAlO_7. Furthermore, our results predict an H—Si distance of 2.22 Å for an Si-(OH) bond and an H—Si distance of 2.36 Å for Si-O_{br}-H. Hence, the difference between Si-(OH) bonds and Si-(O_{br}H)-Al may not be readily distinguishable with CP NMR. The broad distribution of H—Si distances observed in the KOHN et al. (1992) spectra may be due to the fact that the glasses contain over 50 mol% water. At this concentration, $[H_2O]_{mol}$ dominates the ^1H concentration and will be less tightly bound to the aluminosilicate framework structure giving a broader distribution of distances. CP MAS NMR spectroscopy on glasses with water contents of less than 20 mol% would be much better for resolving the H—Si distances with respect to $(OH)^-$ groups because $(OH)^-$ is the dominant species at these concentrations (STOLPER, 1982).

KOHN et al. (1989) suggested that the solution of H_2O in albite glass occurs solely by the exchange of H^+ for Na^+ at the charge-balancing site and formation of NaOH or $[Na(H_2O)_n]^+$ "complexes." However, the KOHN et al. (1989) data also show that the mean nuclear quadrupole coupling constant (C_q) of ^{23}Na remains unchanged in the NMR spectra below total water contents of 30 mol%. KOHN et al. (1989) explain the change in C_q as coordination of Na^+ by molecular H_2O. They state that $(H_2O)_{mol}$ only becomes significant at 30 mol% total H_2O in the model of STOLPER (1982), but this is not the case. $(H_2O)_{mol}$ becomes the *dominant* species relative to $(OH)^-$ above 30 mol% total H_2O, but it is *significant* at much lower total H_2O concentrations. For example, at 13 mol% total H_2O, ≈20% of the water is in the form of $(H_2O)_{mol}$ (IHINGER, 1991). In addition, the charge density distributions and EFG's around Na^+ nuclei in charge-balancing sites are distinctly different from Na^+ nuclei in NaOH or $[Na(H_2O)_n]^+$ complexes (Table 2). If NaOH or $[Na(H_2O)_n]^+$ were forming below 30 mol% total H_2O, significant changes in C_q would be expected and are not observed. For these reasons, we conclude that Na^+ → NaOH (or $[Na(H_2O)_n]^+$) is not a part of the solution mechanism below 30 mol% H_2O.

Proposed Model

From the evidence given above, it is likely that the water solubility mechanism in hydrous aluminosilicate glasses does not involve silicon and that sodium is involved only at water concentrations > 30 mol% H_2O. However, the 900 cm^{-1} Raman peak and features of the ^{27}Al MAS NMR spectra of these hydrous melts cannot be assigned to Al Q^3-(OH) sites unequivocally.

At this point, predictions based on MO calculations of aluminosilicate clusters become helpful. Figure 4 shows that Al-(OH) stretches are common between 800 and 900 cm^{-1} in $[H_6SiAlO_7]^{1-}$ and $[H_6Al_2O_7]^{2-}$ dimers. Furthermore, the predicted frequency shifts of these modes upon deuteration of the cluster can be small (Appendix A) with concomitant decreases in the intensities of the Raman- and IR-active modes. For example, the 825 cm^{-1} vibration in $[H_6SiAlO_7]^{1-}$ shifts 20 cm^{-1} to 805 cm^{-1}, and the Raman and infrared intensities drop from 1.21 and 150.4 to 0.71 and 115.8, respectively. Within the broad Raman and infrared spectra of hydrous albite glass, this small an isotopic frequency shift may not be detected for an Al-(OH) stretch, especially when accompanied by the decrease in intensity. The presence of approximately 0.65 wt% H_2O in the deuterated sample could also hinder detection of an isotopic frequency shift. Isotopic shifts in the glass may be even smaller than those calculated

in the molecules because the Al^{3+} ions in the glass are part of the semi-rigid framework structure (i.e., Q^3; FREUND, 1982); whereas in the molecule, Al^{3+} is bonded to one bridging and two other non-bridging oxygen atoms (i.e., Q^1). Although frequency shifts have not been detected, a decrease in the intensity of the 900 cm^{-1} feature is observed in the infrared (Fig. 1) and Raman spectra (MCMILLAN et al., 1993).

We preclude the possibility of Al-(OH) stretches in $Al(OH)_3$ contributing to the 900 cm^{-1} peak because the most intense Raman frequency of these modes (720 cm^{-1}) is much lower in frequency than the modes in the aluminosilicate dimers. In addition, the intensities of both the Raman- and infrared-active modes in $Al(OH)_3$ increase upon deuteration in contrast to the Al-(OH) modes in the dimers where the intensities decrease. In the infrared (Fig. 1) and Raman (MCMILLAN et al., 1993) spectra, the intensity of the 900 cm^{-1} band decreases with deuteration. An increase in the intensity of the ^{27}Al MAS NMR spectra of the hydrous glass from the dry glass at chemical shifts near 90 ppm would also be expected, if $Al(OH)_3$ molecular units were being formed (BEN et al., 1991). Because there is no apparent change in the NMR intensity near 90 ppm (KOHN et al., 1989), we conclude that no molecular $Al(OH)_3$ is forming. In addition, the formation of $Al(OH)_3$ "clusters" (i.e., $^{[6]}Al^{3+}$) would result in increased intensities near 0 ppm (MULLER et al., 1981; SATO et al., 1991) which is not observed (KOHN et al., 1989). Although $^{[6]}Al^{3+}$, $^{[4]}Al^{3+}$ and $^{[3]}Al^{3+}$ exhibit a range of NMR shifts, in general there is no overlap of NMR shifts between these coordination states (MULLER et al., 1981; BEN et al., 1991; SATO et al., 1991).

The model proposed here for the H_2O solubility mechanism in albite melts is based on the reactions

$$H_2O + 2NaAlSi_3O_8 \Leftrightarrow 2NaAl(OH)Si_3O_{7.5} \quad \text{for} \quad [H_2O]_{tot} < 30 \text{ mol\%}$$

and

$$H_2O + NaAlSi_3O_8 \Leftrightarrow NaOH + HAlSi_3O_8 \quad \text{for} \quad [H_2O]_{tot} > 30 \text{ mol\%}.$$

The first reaction occurs until approximately ¼ to ⅓ of all the Al^{3+} ions in the melt are Q^3 with one Al-(OH) bond. H_2O may preferentially attack Al^{3+} in sites within the melt where the Al-avoidance principle is violated, such as 3-membered rings (KUBICKI and SYKES, 1993a). The second reaction occurs as a rapid exchange of H^+ for Na^+ in charge-balancing sites at high water contents.

It is possible that $[Na(H_2O)_n]^+$ complexes could give rise to the increase in C_q above 30 mol% $[H_2O]_{tot}$ because the EFG of this species is more assymmetric than that of Na(OH) (Table 2). However, this possibility does not explain the existence of three distinctly different H sites in the glass determined from MAS NMR spectra (BEZMEN et al., 1991). Further, if the reaction is solvation of the Na^+ cation, the abrupt change in C_q at 30 mol% $[H_2O]_{tot}$ (KOHN et al., 1989) would not be expected; a gradual increase in $(H_2O)_{mol}$ with increasing $[H_2O]_{tot}$ would result in progressive hydration of the Na^+ cation and affect C_q continuously. In addition, it has been shown that H^+ exchanges with Na^+ in the charge-balancing site of crystalline albite (PAULUS and MULLER, 1988). Hence, we consider the reaction, $H_2O + Na^+ \Leftrightarrow NaOH + H^+$, to be the most probable in the melt at $[H_2O]_{tot}$ concentrations above 30 mol%. Size constraints in the charge-balancing site would favor the reactants in the above reaction, however, so NaOH would remain a minor constituent of the melt. These reactions also explain the observations of IHINGER (1991) on quench rate dependence of $[OH^-]$ concentrations. The $[OH^-]$ concentration in hydrous albite glasses has been shown to be quench rate dependent above 30 mol% $[H_2O]_{tot}$ (IHINGER, 1991). Below this threshold value, however, the $[OH^-]$ is not significantly affected by quench rate. Hence, we conclude that there are two separate bonding sites for $(OH)^-$ in the melt. The first is strongly bound Al-(OH) and does not exchange rapidly with the $(H_2O)_{mol}$ in the system; the second is more weakly bound (NaOH) and exchanges readily with $(H_2O)_{mol}$.

The solubility mechanism proposed above is consistent with all available spectroscopic data on hydrous albite glass. Raman and infrared spectra of H_2O-albite glass differ from the anhydrous glass by the peak near 900 cm^{-1}, the H_2O bend at 1635 cm^{-1}, and the O-H stretches around 3600 cm^{-1}. With the equilibrium reaction between H_2O and Al-(OH), all of these vibrations can be assigned. The NMR shift of ^{29}Si is insignificant with hydration of the glass, which precludes the possibility that Si Q^2 units are formed (MYSEN and VIRGO, 1986b). The ^{27}Al MAS NMR spectrum shows a small shift ($\approx$2.5 ppm) with addition of H_2O to the melt (KOHN et al., 1989). In addition, narrowing of the NMR peak occurs. Both of these observations can be explained by the presence of Al^{3+} in two sites: one an Al Q^4 site and another an Al Q^3 site with one Al-(OH) bond. As a consequence, we suggest that the Q^3 sites have smaller EFG's than the Q^4 sites. OESTRIKE and KIRKPATRICK (1988) and STEBBINS et al. (1991) have shown that ^{27}Al linewidths are narrower in depolymerized aluminosilicate glasses than in fully polymerized aluminosilicate glasses, in contrast to the assumption of KOHN et al. (1989) that the development of Al Q^3 sites would give rise to broader ^{27}Al linewidths.

The chemical shift of an Al Q^3-(OH) site is not expected near 70 ppm, as suggested by KOHN et al. (1989), because of the intermediate bond strength of Al-(OH) with respect to Al-O-*M* and Al-O-*T*. The chemical shift of the Q^3-(OH) site may be similar to that of a Q^4 site because the two bonds on each oxygen have bond orders = 1. Furthermore, GIBBS (1982) has demonstrated that terminal O-H bonds in molecules can successfully mimic the effects of an external silicate network. DOVESI et al. (1987) have shown that the electronic structure surrounding Si in $H_6Si_2O_7$ is nearly identical to that in α-quartz. Hence, *T*-(OH) bonds may be similar to *T*-O-*T* bonds and have similar isotropic chemical shifts. For example, the ^{29}Si chemical shift of Si Q^3-(OH) is closer to the Si Q^4 chemical shift than the Si Q^3-(OM) (FARNAN et al., 1987) chemical shift. Therefore, a significant decrease in the ^{27}Al quadrupole coupling constant combined with a small increase in the ^{27}Al chemical shift dispersion can account for the observed changes in the ^{27}Al MAS NMR spectra.

Solubility by formation of Al-(OH) is also consistent with the viscosity data for hydrous albite melts. Viscosities decrease dramatically with addition of H_2O up to 30 mol% $[H_2O]_{tot}$ (DINGWELL, 1987). Above this water content, the slope of

the viscosity vs. H_2O concentration begins to level off (DINGWELL, 1987). The three orders of magnitude drop in viscosity is similar to that observed with addition of $[F_2O]^-$ and Na_2O (DINGWELL, 1987) where it is known that depolymerization of the melt is taking place (SCHALLER et al., 1992). ZHANG et al. (1991) have calculated that molecular water diffuses independent of and more rapidly than $(OH)^-$ in rhyolitic melts; hence, molecular H_2O and $(OH)^-$ are decoupled in the melt. $(H_2O)_{mol}$ will not affect the framework structure of the melt as strongly as $(OH)^-$ does by depolymerization. The activation energy of diffusion in silicate melts for $(H_2O)_{mol}$ is similar to that of argon (CARROLL and STOLPER, 1991; ZHANG et al., 1991). Thus, the interaction energetics of $(H_2O)_{mol}$ with the aluminosilicate framework is minimal. Therefore, $(H_2O)_{mol}$ does not dramatically affect the melt structure and cannot cause the observed decrease in viscosity.

If the reactions proposed here do occur, Si-O-Al bonds may be broken. It may be expected that these reactions could induce significant changes in ^{29}Si NMR spectra that are not observed (KOHN et al., 1989). Hence, we examine the possible consequences of Al-(OH) formation on the chemical environment of the Si^{4+} cation. Si Q^2 sites are not forming because this would result in significant shifts, to more positive values, in the ^{29}Si MAS NMR peak position (MURDOCH et al., 1985; KOHN et al., 1989). A small number of Q^3 Si-(OH) bonds may form because there appears to be a slight increase in Raman intensity near 970 cm^{-1} apparent in the hydrous albite glass spectra (MCMILLAN et al., 1993). If this is true, then it may be argued that a shift in the NMR spectrum of ^{29}Si should be detected because there is a 10 ppm difference in the ^{29}Si NMR chemical shift between Si Q^4 and Si Q^3-(OH). In the hydrous albite melt, the actual reaction is closer to $[Si(OSi)_3(OAl)] \rightarrow [Si(OSi)_3(OH)]$. The NMR shifts for Si Q^4-(nAl) scale linearly with the number of Al^{3+} next nearest neighbors (LIPPMAA et al., 1980, 1981; OESTRIKE et al., 1987; SHERRIFF and GRUNDY, 1988), so a 5 ppm shift is reasonable for $[Si(OSi)_3(OAl)] \rightarrow [Si(OSi)_3(OH)]$. Because only $^1/_3$ of all Al^{3+} ions may form Al-(OH) bonds, only $^1/_9$ of all Si^{4+} ions need to form Si-(OH) bonds. Therefore, the total shift in the ^{29}Si NMR spectra of hydrous albite glass may only be 0.5 ppm. Such a small change may not be detectable, especially when other structural rearrangements are taking place between anhydrous and hydrous glasses.

If Al-O-Al linkages preferentially react with H_2O, no change is necessary in the ^{29}Si MAS NMR spectra (SYKES and LUTH, 1990; KUBICKI and SYKES, 1993a). Although albite glasses are generally ordered with respect to Al-O-Si linkages (MURDOCH et al., 1985), a percentage of Al^{3+} ions may violate the Al-avoidance principle (LOWENSTEIN, 1954) in albite melts at high temperatures because the enthalpy of mixing is only −22.6 kJ/mol in this system (NAVROTSKY et al., 1982). Al-O-Al linkages have been detected in anorthite crystals annealed at 1400°C (PHILLIPS et al., 1992), so it is likely that they exist in glasses as well. KUBICKI and SYKES (1993a) have demonstrated the existence of aluminosilicate 3-membered rings and their association with the 580 cm^{-1} peak in albite glass. The presence of 3-membered rings increases the likelihood of Al-O-Al linkages in aluminosilicate glasses. The 3-membered rings have associated high strain energies and may be preferred sites for attack by H_2O. Hence, it is not necessary to assume any change occurs in the local Si environment with the formation of Q^3 Al-(OH). Such a preference of H_2O for Al-O-Al linkages would help to explain the transition between $(OH)^-$ and H_2O-dominated speciation in the albite melt (STOLPER, 1982) as the Al-O-Al linkages are eliminated, water would tend to remain associated as $(H_2O)_{mol}$. This is our preferred mechanism for the reaction of H_2O with albite melts to form Al-(OH) bonds.

CONCLUSIONS

Water entering into albite melts initially forms Al-(OH) bonds and a lesser amount of molecular H_2O. The Al-(OH) bonds give rise to a peak near 900 cm^{-1} in the vibrational spectra of hydrous albite glasses. Frequency shifts from the isotopic substitution of deuterium for hydrogen are not detectable in vibrational spectra because the shifts are small, Al-(OD) peak intensities decrease, and Al-(OH) was not eliminated from the melt. At 30 mol% $[H_2O]_{tot}$, $(H_2O)_{mol}$ becomes the dominant H-bearing species as the reactive Al^{3+} sites are consumed. Protons exchange with Na^+ in the charge-balancing sites and form NaOH. The presence of NaOH is detected by the sharp rise in C_q for ^{23}Na in NMR spectra and possibly by a 635 cm^{-1} peak in the Raman spectra of high water content albite glasses. Size constraints of the charge-balancing sites favor the presence of Na^+; thus, $(H_2O)_{mol}$ remains the dominant species for hydrogen above 30 mol% $[H_2O]_{tot}$ and NaOH is a minor percentage of total Na in the glass.

Acknowledgments—The authors gratefully acknowledge the prompt and thorough reviews of S. C. Kohn and an anonymous reviewer. We appreciate the critical comments of G. R. Rossman on an earlier version of this manuscript and for the use of the infrared spectrometer. J. D. Kubicki also acknowledges the support of the Schlumberger Corporation and NSF grants EAR91-17946 (G. A. Blake) and EAR91-54186 (E. M. Stolper). Dan Sykes acknowledges support from the Earth Sciences section of the U.S. National Science Foundation, Grant EAR89-04375 (P. J. Wyllie). Computational facilities were provided by the Molecular Simulation Center (W. A. Goddard) of the Beckman Institute at Caltech, the Pittsburgh Supercomputing Center, and E. M. Stolper.

Editorial handling: P. C. Hess

REFERENCES

ANDZELM J. and WIMMER E. (1991) DGauss—a density functional method for molecular and electronic structure calculations in the 1990's. *Physica* **B 172,** 307–317.

BEN R., JANSSEN E., LEHMKUHL H., RUFINSKA A., ANGERMUND K., BETZ P., GODDARD R., and KRUGER C. (1991) Drei- oder vierfach-koordination des aluminiums in alkylaluminiumphenoxiden und deren unterscheidung durch ^{27}Al-NMR-spektroskopie. *J. Organomet. Chem.* **41,** 37–55.

BEZMEN N. I., ZHARIKOV V. A., EPELBAUM M. B., ZAVELSKY V. O., DIKOV Y. P., SUK N. I., and KOSHEMCHUK S. K. (1991) The system $NaAlSi_3O_8$-H_2O-H_2 (1200°C, 2 kbar): The solubility and interaction mechanism of fluid species with melt. *Contrib. Mineral. Petrol.* **109,** 89–97.

BLINC R. (1976) Magnetic resonance studies of hydrogen bonding in solids. In *The Hydrogen Bond: Recent Developments in Theory and Experiments. II. Structure and Spectroscopy* (ed. P. SCHUSTER et al.), Vol. 2, Chap. 18, pp. 831–887. North-Holland.

BOYD F. R. and ENGLAND J. (1960) Apparatus for phase-equilibrium measurements at pressures up to 50 kb and temperatures up to 1750°C. *J. Geophys. Res.* **65,** 741–748.

BURKHARD D. J. M., DE JONG B. H. W. S., MEYER A. J. H. M., and VAN LENTHE J. H. (1991) $H_6Si_2O_7$: Ab initio molecular orbital calculations show two geometric conformations. *Geochim. Cosmochim. Acta* **55,** 3453–3458.

CARROLL M. R. and STOLPER E. M. (1991) Argon solubility and diffusion in silica glass: Implications for the solution behavior of molecular gases. *Geochim. Cosmochim. Acta* **55,** 211–225.

DINGWELL D. B. (1987) Melt viscosities in the system $NaAlSi_3O_8$-H_2O-F_2O_{-1}. In *Magmatic Processes: Physicochemical Principles.* (ed. B. O. MYSEN); *Special Publication No. 1,* pp. 423–431. The Geochemical Society.

DINGWELL D. B. and MYSEN B. O. (1985) Effects of fluorine and water on the viscosity of albite melt at high pressure: A preliminary investigation. *Earth Planet. Sci. Lett.* **74,** 266–274.

DOVESI R., PISANI C., ROETTI C., and SILVI B. (1987) The electronic structure of α-quartz: A periodic Hartree-Fock calculation. *J. Chem. Phys.* **86,** 6967–6971.

DOWTY E. (1990) *Atoms. A Computer Program For Displaying Atomic Structures.* Eric Dowty, Kingsport, TN.

DUPREE R., HOLLAND D., MCMILLAN P. W., and PETTIFER R. F. (1984) The structure of soda-silica glasses: A MAS NMR study. *J. Non-Cryst. Solids* **68,** 399–410.

ENGELHARDT G. and MICHEL D. (1987) *High-resolution Solid-state NMR of Silicates and Zeolites.* Wiley.

FARNAN I., KOHN S. C., and DUPREE R. (1987) A study of the structural role of water in hydrous silica glass using cross-polarisation magic angle spinning NMR. *Geochim. Cosmochim. Acta* **51,** 2869–2874.

FREUND F. (1982) Solubility mechanisms of H_2O in silicate melts at high pressures and temperatures: A Raman spectroscopic study: Discussion. *Amer. Mineral.* **67,** 153–154.

FRISCH M. J., HEAD-GORDON M., TRUCKS G. W., FORESMAN J. B., SCHLEGEL H. B., RAGHAVACHARI K., ROBB M., BINKLEY J. S., GONZALEZ C., DEFREES D. J., FOX D. J., WHITESIDE R. A., SEEGER R., MELIUS C. F., BAKER J., MARTIN R. L., KAHN L. R., STEWART J. J. P., TOPIOL S., and POPLE J. A. (1990) *Gaussian 90,* Revision I. Gaussian, Inc.

FURUKAWA T., FOX K. E., and WHITE W. B. (1981) Raman spectroscopic investigation of the structure of silicate glasses. III. Raman intensities and structural units in sodium silicate glasses. *J. Chem. Phys.* **75,** 3226–3237.

GALEENER F. L. and MIKKELSON J. C., JR. (1982) Vibrational dynamics in ^{18}O-substituted vitreous silica. *Phys. Rev.* **B 23,** 5527–5530.

GEISINGER K. L., GIBBS G. V., and NAVROTSKY A. (1985) A molecular orbital study of bond length and angle variations in framework structures. *Phys. Chem. Mineral.* **11,** 266–283.

GIBBS G. V. (1982) Molecules as models for bonding in silicates. *Amer. Mineral.* **67,** 421–450.

HESS A. C., MCMILLAN P. F., and O'KEEFFE M. (1986) Force fields for SiF_4 and H_4SiO_4: Ab initio molecular orbital calculations. *J. Phys. Chem.* **90,** 5661–5665.

HILL J.-R. and SAUER J. (1989) Harmonic force constants of the H_3Si-O-AlH_3 anion—A model of Si-O-Al bonds in aluminosilicates. *Z. Phys. Chemie* **270,** S203–206.

IHINGER P. D. (1991) An experimental study of the interaction of water with granitic melt. Ph.D. dissertation, California Inst. Tech.

KINSEY R. A., KIRKPATRICK R. J., HOWER J., SMITH K. A., and OLDFIELD E. (1985) High resolution aluminum-27 and silicon-29 nuclear magnetic resonance spectroscopic study of layer silicates, including clay minerals. *Amer. Mineral.* **70,** 537–548.

KOHN S. C., DUPREE R., and SMITH M. E. (1989) A multinuclear magnetic resonance study of the structure of hydrous albite glasses. *Geochim. Cosmochim. Acta* **53,** 2925–2935.

KOHN S. C., DUPREE R., and MORTUZA M. G. (1992) The interaction between water and aluminosilicate magmas. *Chem. Geol.* **96,** 399–409.

KUBICKI J. D. and SYKES D. (1993a) Molecular orbital calculations of vibrations in three-membered aluminosilicate rings. *Phys. Chem. Mineral.* (in press).

KUBICKI J. D. and SYKES D. (1993b) Molecular orbital calculations on $H_6Si_2O_7$ with variable Si-O-Si angle: Implications for the high-pressure vibrational spectra of silicate glasses. *Amer. Mineral.* (in press).

KUMMERLEN J., MERWIN L. H., SEBALD A., and KEPPLER H. (1992) Structural role of H_2O in sodium-silicate glasses—results from Si-29 and H-1 NMR spectroscopy. *J. Phys. Chem.* **96,** 6405–6410.

LASAGA A. C. and GIBBS G. V. (1988) Quantum mechanical potential surfaces and calculations on minerals and molecular clusters. *Phys. Chem. Mineral.* **16,** 29–41.

LASAGA A. C. and GIBBS G. V. (1991) Quantum mechanical Hartee-Fock potential surfaces and calculations on minerals. II. 6-31G* results. *Phys. Chem. Mineral.* **17,** 485–491.

LIPPMAA E., MAGI M., SAMOSON A., ENGELHARDT G., and GRIMMER A. (1980) Structural studies of silicates by solid-state high-resolution ^{29}Si NMR. *J. Amer. Chem. Soc.* **102,** 4889–4893.

LIPPMAA E., MAGI M., SAMOSON A., TARMAK M., and ENGELHARDT G. (1981) Investigation of the structure of zeolites by solid-state high-resolution ^{29}Si NMR spectroscopy. *J. Amer. Chem. Soc.* **103,** 4992–4996.

LOWENSTEIN W. (1954) The distribution of aluminum in the tetrahedra of silicates and aluminates. *Amer. Mineral.* **39,** 92–96.

MATSON D. W., SHARMA S. K., and PHILPOTTS J. A. (1983) The structure of high-silica alkali-silicate glasses. A Raman spectroscopic investigation. *J. Non-Cryst. Solids* **58,** 323–352.

MCMILLAN P. F. (1984) Structural studies of silicate glasses and melts—Applications and limitations of Raman spectroscopy. *Amer. Mineral.* **69,** 622–644.

MCMILLAN P. F. (1989) Raman spectroscopy in mineralogy and geochemistry. *Ann. Rev. Earth Planet. Sci.* **17,** 255–283.

MCMILLAN P. F. and REMMELE R. L. (1986) Hydroxyl sites in SiO_2 glass: A note on infrared and Raman spectra. *Amer. Mineral.* **71,** 772–778.

MCMILLAN P. F., JAKOBSSON S., HOLLOWAY J. R., and SILVER L. A. (1983) A note on the Raman spectra of water-bearing albite glasses. *Geochim. Cosmochim. Acta* **47,** 1937–1943.

MCMILLAN P. F., STANTON T. R., POE B. T., and REMMELE R. L. (1993) A Raman spectroscopic study of H/D isotopically-substituted hydrous aluminosilicate glasses. *Phys. Chem. Mineral.* (in press).

MERWIN L., KEPPLER H., and SEBALD A. (1991) ^{29}Si MAS NMR evidence for the depolymerization of silicate melts by water. *Eos* **72,** 573 (abstr.).

MOENKE H. H. W. (1974) Silica, the three-dimensional silicates, borosilicates, and beryllium silicates. In *The Infrared Spectra of Minerals* (ed. V. C. FARMER), Monograph No. 4, pp. 383–423. Mineral. Soc. London.

MORTIER W. J., SAUER J., LERCHER J. A., and NOLLER H. (1984) Bridging and terminal hydroxyls. A structural chemical and quantum chemical discussion. *J. Phys. Chem.* **88,** 905–912.

MOZZI R. L. and WARREN B. E. (1969) The structure of vitreous silica. *J. Appl. Crystall.* **2,** 164–172.

MULLER D., GESSNER W., BEHRENS H., and SCHELER G. (1981) Determination of the aluminum coordination in aluminum oxygen compounds by solid-state high-resolution ^{27}Al NMR. *Chem. Phys. Lett.* **79,** 59–62.

MURAKAMI M. and SAKKA S. (1987) Ab initio molecular orbital study on the vibrational spectra of silicate glasses. *J. Non-Cryst. Solids* **95,** 225–232.

MURDOCH J. B., STEBBINS J. F., and CARMICHAEL I. S. E. (1985) High-resolution ^{29}Si MNR study of silicate and aluminosilicate glasses: The effect of network modifying cations. *Amer. Mineral.* **70,** 332–343.

MYSEN B. O. and VIRGO D. (1986a) Volatiles in silicate melts at high pressure and temperature 1. Interaction between OH groups and Si^{4+}, Al^{3+}, Ca^{2+}, Na^+ and H^+. *Chem. Geol.* **57,** 303–331.

MYSEN B. O. and VIRGO D. (1986b) Volatiles in silicate melts at high pressure and temperature. 2. Water in melts along the join $NaAlO_2$-SiO_2 and a comparison of solubility mechanisms of water and fluorine. *Chem. Geol.* **57,** 333–358.

MYSEN B. O., VIRGO D., HARRISON W., and SCARFE C. (1980) Solubility mechanisms of H_2O in silicate melts at high pressures and temperatures: A Raman spectroscopic study. *Amer. Mineral.* **65,** 900–914.

NAVROTSKY A., PERAUDEAU G., MCMILLAN P. F., and COUTURES J. P. (1982) A thermochemical study of glasses and crystals along the joins silica-calcium aluminate and silica-sodium aluminate. *Geochim. Cosmoshim. Acta* **46,** 2039–2047.

NAVROTSKY A., GEISINGER K. L., MCMILLAN P. F., and GIBBS G. V. (1985) The tetrahedral framework in glasses and melts—Inferences from molecular orbital calculations and implications for structure, thermodynamics and physical properties. *Phys. Chem. Mineral.* **11,** 284–298.

NEWMAN S., STOLPER E. M., and EPSTEIN S. (1986) Measurement of water in rhyolitic glasses: Calibration of an infrared spectroscopic technique. *Amer. Mineral.* **71,** 1527–1541.

OESTRIKE R. and KIRKPATRICK R. J. (1988) ^{27}Al and ^{29}Si MASS NMR spectroscopy of glasses in the system anorthite-diopside-forsterite. *Amer. Mineral.* **73,** 534–546.

OESTRIKE R., YANG W. H., KIRKPATRICK R. J., HERVIG R. L., NAVROTSKY A., and MONTEZ B. (1987) High-resolution ^{23}Na, ^{27}Al, ^{29}Si NMR spectroscopy of framework aluminosilicate glasses. *Geochim. Cosmochim. Acta* **51,** 2199–2209.

PAULUS H. and MULLER G. (1988) The crystal structure of hydrogen-feldspar. *Neues Jahrb. Mineral. Mh.* **11,** 481–490.

PHILLIPS B. L., KIRKPATRICK R. J., and CARPENTER M. A. (1992) Investigation of short-range Al,Si order in synthetic anorthite by ^{29}Si MAS NMR spectroscopy. *Amer. Mineral.* **77,** 484–494.

PICHAVANT M., HOLTZ F., and MCMILLAN P. (1992) Phase relations and compositional dependence of H_2O solubility in quartz-feldspar melts. *Chem. Geol.* **96,** 303–319.

RYSKIN Y. (1974) The vibrations of protons in minerals: Hydroxyl, water and ammonium. In *The Infrared Spectra of Minerals* (ed. V. C. FARMER), pp. 137–181. Mineral. Soc. London.

SATO R. K., MCMILLAN P. F., DENNISON P., and DUPREE R. (1991) High-resolution ^{27}Al and ^{29}Si MAS NMR investigation of SiO_2-Al_2O_3 glasses. *J. Phys. Chem.* **95,** 4483–4489.

SAUER J. (1989) Molecular models in ab initio studies of solids and surfaces: from ionic crystals and semiconductors to catalysts. *Chem. Rev.* **89,** 199–255.

SCHALLER T., DINGWELL D. B., KEPPLER H., KNOLLER W., MERWIN L., and SEBALD A. (1992) Fluorine in silicate glasses: A multinuclear nuclear magnetic resonance study. *Geochim. Cosmochim. Acta* **56,** 701–707.

SHARMA S. K., YODER H. S., and MATSON D. W. (1988) Raman study of some melilites in crystalline and glassy states. *Geochim. Cosmochim. Acta* **52,** 1961–1967.

SHERRIFF B. L. and GRUNDY H. D. (1988) Calculations of ^{29}Si MAS NMR chemical shift from silicate mineral structure. *Nature* **332,** 819–822.

SILVER L. and STOLPER E. M. (1989) Water in albitic glasses. *J. Petrol.* **30,** 667–709.

SILVER L. A., IHINGER P. D., and STOLPER E. M. (1990) The influence of bulk composition on the speciation of water in silicate glasses. *Contrib. Mineral. Petrol.* **104,** 142–162.

STEBBINS J. F., FARNAN I., and FISKE P. (1991) The effects of temperature on silicate liquid structure: A multi-nuclear, high temperature NMR study. *Eos* **72,** 572 (abstr.).

STOLEN R. and WALRAFEN G. (1976) Water and its relation to broken bond defects in fused silica. *J. Chem. Phys.* **64,** 2623–2631.

STOLPER E. M. (1982) Water in silicate glasses: An infrared spectroscopic study. *Contrib. Mineral. Petrol.* **81,** 1–17.

STONE J. and WALRAFEN G. (1982) Overtone vibrations of OH-groups in fused silica optical fibers. *J. Chem. Phys.* **76,** 1712–1722.

SYKES D. and LUTH R. W. (1990) A spectroscopic investigation of the structure of anhydrous and hydrous $KAlSi_3O_8$ glasses quenched from high pressure. *Eos* **71,** 1666 (abstr.).

UCHINO T., IWASAKI M., SAKKA T., and OGATA Y. (1991) Ab initio molecular orbital calculations on the electronic structure of sodium silicate glasses. *J. Phys. Chem.* **95,** 5455–5462.

WILSON E. B., DECIUS J. C., and CROSS P. C. (1955) *Molecular Vibrations—The Theory of Infrared and Raman Vibrational Spectra.* Dover Publications.

WOLFF R., RADEGLIA R., and SAUER J. (1986) Charge differences between silicon atoms in aluminosilicates and their relation to ^{29}Si NMR chemical shifts. A quantum-chemical study. *J. Mol. Struct.* **139,** 113–124.

WOLFF R., RADEGLIA R., VOGEL C., and SAUER J. (1989) Theoretical interpretation of ^{29}Si NMR chemical shifts of aluminosilicates. Part 2. The Si-O-T (T = Si or Al) bond angle dependence. *J. Mol. Struct.* **183,** 223–232.

ZHANG Y., STOLPER E. M., and WASSERBURG G. J. (1991) Diffusion of water in rhyolitic glasses. *Geochim. Cosmochim. Acta* **55,** 441–456.

Appendix A. Frequencies , reduced masses (m), intensities (Raman in Å^4/amu; infrared in KM/mole), and H-D isotopic shifts of vibrational modes from molecular orbital calculations at the 3-21G* level. Vibrational modes are given in order of the dominant displacements that contribute to the mode. Motion codes are in terms of stretches and bends. For example, T-(OH) and O-H denote tetrahedral non-bridging oxygen and hydroxyl stretches, respectively; OTO and TOT denote intratetrahedral bend and intertetrahedral bends, respectively.

Frequency	μ	Motion	Raman	Infrared	H-D shift
Na(OH)					
409.3	1.2	O-H, NaOH	0.04	136.4	100.6
707.6	11.3	Na-O	7.25	56.8	12.7
3863.1	1.1	O-H	227.36	31.3	1045.8
Al(OH)$_3$					
264.5	3.0	O-H, OAlO, AlOH	2.45	56.7	35.8
290.9	2.0	O-H	0.00	29.3	60.2
357.4	1.1	O-H, AlOH	4.24	0.0	90.0
401.0	1.9	O-H, AlOH	0.00	778.0	36.5
511.8	1.2	O-H, AlOH	2.29	0.0	125.4
519.5	1.5	O-H, AlOH	3.37	386.8	88.8
801.9	5.1	Al-(OH), AlOH	4.64	0.0	31.3
1076.0	7.8	Al-(OH), OAlO, AlOH	1.41	163.8	26.9
4037.4	1.1	O-H	65.75	115.0	1092.5
4038.7	1.1	O-H	188.02	0.0	1092.5
[H$_4$AlO$_4$]$^-$					
169.1	1.8	OAlO, O-H	5.44	0.0	35.3
171.3	1.2	O-H, OAlO, AlOH	4.84	23.0	42.0
173.5	2.2	OAlO, O-H, AlOH	1.74	125.7	29.5
296.8	2.2	OAlO, O-H, AlOH	4.53	7.0	46.1
311.0	2.0	OAlO, O-H, AlOH	4.86	0.0	33.0
335.3	3.0	OAlO, O-H, AlOH	1.15	105.1	36.4
419.5	2.9	OAlO, O-H, AlOH	1.54	346.9	29.0
687.3	5.3	Al-(OH), AlOH	2.94	0.0	158.7
738.1	1.2	O-H, AlOH	1.24	0.0	46.6
746.4	1.6	Al-(OH), Al-O-H, AlOH	2.53	254.6	150.3
746.5	1.5	Al-O-H, O-H, AlOH	13.77	257.3	162.8
868.3	4.3	Al-(OH), AlOH, OAlO	2.90	101.4	23.4
905.3	4.2	Al-O-H, OAlO, AlOH	1.79	217.6	28.2
3862.2	1.1	O-H	207.08	0.0	1050.4
3864.2	1.1	O-H	65.24	8.5	1051.7
3864.8	1.1	O-H	132.70	1.3	1052.4

Frequency	μ	Motion	Raman	Infrared	H-D shift
H$_4$SiO$_4$					
158.3	1.4	O-H	4.66	0.0	38.0
185.2	1.7	O-H, OSiO	2.05	245.5	37.7
207.1	1.3	O-H, SiOH	3.63	21.0	38.4
355.4	2.5	OSiO, SiOH	3.08	3.4	49.6
367.0	3.0	OSiO ,O-H, SiOH	0.84	0.0	25.0
417.5	2.8	OSiO, O-H, SiOH	1.55	133.9	48.2
510.3	3.5	OSiO, O-H, SiOH	0.63	385.8	29.8
810.2	12.1	Si-(OH), SiOH	7.00	0.0	4.0
891.4	1.7	Si-O-H, SiOH	6.90	386.1	183.5
895.9	1.8	Si-O-H, SiOH	0.80	348.7	166.2
898.4	1.1	SiOH, O-H	1.19	0.0	244.1
1030.4	3.4	Si-(OH), SiOH, OSiO	3.25	114.5	44.7
1094.5	3.5	Si-O-H, Si-(OH), SiOH	1.47	286.2	54.0
3965.8	1.1	O-H	39.59	118.0	1079.5
3966.0	1.1	O-H	90.23	52.9	1080.2
3970.0	1.1	O-H	153.26	0.0	2890.4

Frequency	μ	Motion	Raman	Infrared	H-D shift
H$_6$Si$_2$O$_7$					
45.2	6.6	SiOSi, OSiO	0.11	0.4	2.1
48.7	6.8	SiOSi, OSiO SiOH	0.01	2.3	5.4
136.8	5.7	SiOSi, OSiO	0.55	6.2	10.9
181.5	1.4	O-H, OSiO, SiOH	2.77	133.0	38.9
201.3	1.5	O-H, OSiO	2.65	63.5	46.3
207.4	2.0	OSiO, O-H	2.93	137.4	38.9
223.1	1.6	O-H, OSiO	4.12	52.4	45.6
253.7	1.6	O-H, OSiO, SiOH	2.74	25.9	59.0
272.0	2.6	OSiO, O-H, SiOH	1.49	13.8	17.0

Appendix A (Continued)

294.0	2.5	O-H, OSiO, SiOH	1.72	27.2	31.2
338.4	2.7	O-H, OSiO, SiOH	0.70	70.7	40.7
362.0	3.3	OSiO, O-H, SiOH	0.66	113.7	32.7
382.1	2.7	OSiO, O-H, SiOH	2.67	53.2	41.6
408.3	2.8	OSiO, O-H, SiOH	1.33	168.6	41.9
412.5	3.0	OSiO, O-H, SiOH	1.40	37.1	45.0
448.8	4.3	OSiO, O-H, SiOH	1.12	85.6	24.9
477.0	4.1	OSiO, SiOSi, O-H	1.27	145.1	46.2
485.9	4.4	SiOSi, OSiO, O-H	1.61	115.6	43.4
659.1	1.2	O-H, SiOH	2.67	179.3	146.1
709.4	3.8	Si-O_{br}, SiOSi, Si-(OH)	4.24	271.6	26.7
775.7	1.4	Si-O-H, SiOH	4.26	292.4	23.4
790.8	1.5	SiOH, O-H	3.16	539.4	180.8
796.5	1.8	SiOH, Si-O-H	4.67	232.4	180.0
800.2	1.3	SiOH, O-H	2.68	88.8	173.2
869.5	2.0	Si-O-H, SiOH	2.17	117.4	228.0
922.9	2.8	Si-(OH), SiOH	0.58	114.5	32.9
1003.7	1.5	Si-(OH), O-H, SiOH	6.01	435.6	221.7
1028.3	7.4	Si-O_{br}, SiOSi, Si-(OH)	1.80	290.9	19.3
1080.1	6.7	Si-O_{br}, Si-(OH), SiOH	0.63	63.6	24.1
1110.1	6.0	Si-(OH), OSiO, SiOH	1.90	3.9	28.3
1132.2	6.7	Si-(OH), OSiO, SiOH	0.84	479.9	29.4
1154.5	3.6	SiOSi, Si-(OH), OSiO	3.45	163.5	40.3
1255.1	13.7	Si-O_{br}, SiOSi, OSiO	0.29	850.4	3.8
3857.6	1.1	O-H, SiOH	59.89	258.5	1048.9
3974.7	1.1	O-H	86.75	128.9	1078.8
3981.9	1.1	O-H, SiOH	72.29	109.7	1080.1
3986.4	1.1	O-H	84.55	97.9	1081.5
3994.3	1.1	O-H	56.88	171.3	1083.1
3995.1	1.1	O-H	158.30	47.0	1083.0

Frequency	μ	Motion	Raman	Infrared	H-D shift
$[H_6SiAlO_7]^{1-}$					
34.3	7.3	OTO	0.14	1.5	1.3
47.7	8.0	OAlO, TOT, TOH	0.13	2.0	1.6
150.3	2.2	(Al) O-H, OAlO	1.74	88.3	26.1
164.2	1.9	(Al) O-H, OAlO, AlOH	3.35	20.1	33.1
179.3	1.6	(Al) O-H, OAlO, AlOH	4.78	27.9	39.4
194.5	1.4	(Si) O-H, OSiO, TOH	3.55	73.7	49.0
213.5	2.1	(Si) O-H, OTO, SiOH	2.57	69.6	34.9
230.6	2.7	(Si) O-H, OTO, TOH	1.83	90.2	23.6
248.8	2.3	(Al) O-H, OTO, TOH	3.74	29.8	23.5
277.9	2.6	O-H, OTO, TOH	1.71	6.9	27.9
301.2	1.6	O-H, OTO, TOH	3.75	164.4	49.4
323.9	2.2	OTO, (Si) O-H, TOH	1.72	72.2	39.6
330.6	5.1	TOT, OTO, (Al) O-H	1.90	41.3	18.2
360.9	3.0	OTO, (Al) O-H, TOH	0.85	28.9	35.6
378.5	5.4	OTO, (Al) O-H, TOH	0.88	90.6	29.2
387.5	3.6	OTO, (Si) O-H, TOH	1.84	63.8	19.5
462.5	7.2	OTO, TOH	0.93	172.6	21.4
480.7	6.9	OTO, TOT, TOH	0.22	43.3	19.7
649.6	6.8	T-O_{br}, TOT, Al-O-H	4.45	82.3	42.6
695.9	1.4	Al-(OH), (Al) O-H, AlOH	1.99	147.3	165.4
703.1	1.4	Al-(OH), (Al) O-H, AlOH	6.91	262.2	147.7
746.5	4.0	Al-O_{br}, TOT, Al-O-H	0.97	214.1	89.7
809.4	1.6	Al-(OH), (Al) O-H, AlOH	4.14	183.4	123.5
860.2	3.5	Al-(OH), Si-O-H, TOH,	3.23	113.9	152.5
874.6	2.6	Al-(OH), (Si) O-H, TOH	2.69	243.7	28.0
905.1	2.0	O-H, T-(OH), SiOH	3.05	102.0	133.1
917.3	2.1	Al-(OH), (Al) O-H, TOH	1.21	150.4	23.4
938.6	4.0	T-(OH), TOH, Si-O-H	2.76	184.2	33.4
1004.4	1.4	Si-(OH), (Si) O-H, TOH	0.63	62.1	261.5
1060.2	3.6	Si-(OH), Si-O-H, TOT	0.80	406.8	62.3
1101.3	5.0	T-O_{br}, Si-(OH), OSiO	1.30	369.1	72.1
1175.4	8.9	T-O_{br}, Si-(OH), OTO	1.24	330.3	94.4
1353.7	1.1	(Si) O-H, SiOH, OSiO	4.85	486.2	170.1
3373.5	1.1	(Si) O-H	68.45	827.6	914.9
3906.8	1.1	(Al) O-H, AlOH	134.23	0.5	1062.0
3907.5	1.1	(Al) O-H	93.40	1.3	1062.4
3933.6	1.1	(Al) O-H, AlOH	128.08	4.4	1069.6
3943.5	1.1	(Si) O-H	93.67	27.7	1072.4
3948.1	1.1	(Si) O-H	72.66	43.4	1073.7

Frequency	μ	Motion	Raman	Infrared	H-D shift
$[H_7SiAlO_7]^a$					
37.3	6.74	OTO, TOH	1.05	0.07	0.1
48.9	6.63	TOT, OTO, TOH	0.08	0.87	0.2
148.4	4.14	OTO, TOH	0.49	10.22	2.3
179.1	1.44	OTO, TOH	3.19	104.45	0.2
184.7	5.82	TOT, OTO, TOH	0.61	2.33	0.6
202.6	2.28	TOT, OTO, TOH	1.72	7.19	1.4
229.3	1.57	TOT, OTO, TOH	2.27	79.82	0.7
244.2	2.84	TOT, OTO, TOH	2.29	20.80	0.7
260.5	2.58	TOT, OTO, TOH	1.31	1.52	1.0
281.8	1.78	OTO, TOH	1.14	226.88	6.4
312.0	3.73	TOT, OTO, TOH	2.08	23.93	11.1
330.6	2.22	OTO, TOH	2.56	99.14	6.1
353.3	3.23	OTO, TOH	1.33	395.76	1.6
375.5	1.47	OTO, TOH	4.25	109.51	2.9
397.4	2.10	OTO, TOH	2.85	84.65	15.4
403.2	2.22	TOT, OTO, TOH	0.88	87.21	6.0
421.7	3.33	O_{br}-H, OTO, TOH	1.31	43.62	6.5
457.8	4.01	TOT, OTO, TOH	1.16	9.00	1.3
549.5*	1.57	Al-O_{br}, O-H, TOT, AlOH	3.26	291.98	12.7
567.5	1.49	O-H, TOT, AlOH	4.08	34.53	10.2
603.8*	3.01	Al-O_{br}, O-H, TOT, OTO, TOH	1.48	238.37	37.2
651.3	1.57	O_{br}-H, OTO, TOH	1.90	175.15	57.3
740.1*	1.65	(T-O_{br}), Si-O-H, Al-O, SiOH	2.78	235.31	13.2
748.8	3.65	Al-O, O-H, TOH	3.72	82.07	0.3
780.7	1.40	Si-O-H, SiOH	2.70	359.15	7.7
831.8	1.29	O-H, TOH	3.44	195.84	37.8
850.9*	5.44	T-O_{br}, Si-(OH), TOT, OTO, TOH	4.06	31.91	18.3
926.8	5.95	Al-(OH), TOT, OAlO, TOH	1.08	185.91	9.2
988.0*	4.96	Si-O_{br}, T-(OH), OTO, TOH	1.13	161.23	33.7
992.8	5.01	Al-(OH), TOT, OTO, TOH	1.06	82.71	3.6
1037.8	1.24	O-H, SiOH	0.68	254.57	32.6
1130.3	3.58	Si-(OH), O_{br}-H, OSiO, TOH	1.93	331.06	92.6
1155.2	2.99	Si-(OH), O_{br}-H, TOT, OSiO, TOH	1.12	331.31	18.9
1213.9	2.20	Si-(OH), O_{br}-H, TOT, OSiO, TOH	0.27	428.27	28.1
1353.6	1.12	O-H, SiOH	6.06	509.37	0.5
3179.7	1.07	O-H, SiOH	74.56	1305.35	370.5
3861.9	1.06	O-H, TOH	40.32	237.56	682.2
3963.2	1.07	O-H, AlOH	104.85	46.25	0.0
3986.2	1.07	O-H, SiOH	76.22	134.05	0.0
4006.7	1.07	O-H	106.22	44.36	0.0
4011.4	1.07	O-H, SiOH	107.15	141.91	0.0
4023.8	1.07	O-H, AlOH	117.78	42.35	0.0

a - Deuterium substitution on the H-O_{br} only

Frequency	μ	Motion	Raman	Infrared	H-D shift
$[H_6Al_2O_7]^{2-}$					
29.7	6.9	OAlO, AlOAl	0.07	1.7	1.3
33.7	9.6	OAlO	0.05	2.1	0.7
138.4	7.4	AlOAl, OAlO, O-H	0.52	10.4	5.9
155.9	1.8	O-H, OAlO	0.75	0.5	33.6
171.5	4.0	AlOAl, OAlO, O-H	1.50	3.9	15.6
190.0	2.4	OAlO, O-H	4.44	22.1	29.6
211.9	3.7	OAlO, O-H	0.26	38.0	21.0
230.5	3.0	OAlO, O-H	0.24	18.5	16.8
265.6	2.2	OAlO, O-H	1.53	12.4	47.2
288.6	1.6	OAlO, O-H	1.83	44.1	65.7
291.2	2.8	OAlO, O-H	1.44	13.7	49.8
300.4	1.5	OAlO, O-H	5.54	38.6	38.5
315.2	4.4	OAlO, O-H	1.99	15.4	43.2
327.3	2.1	OAlO, O-H	5.77	15.3	30.5
356.5	2.1	OAlO, O-H	4.12	69.9	32.9
391.4	2.9	OAlO, O-H	2.68	361.6	28.3
408.9	3.4	OAlO, O-H	0.72	241.9	28.5
446.8	2.7	OAlO, O-H	1.91	109.4	32.4
604.9	7.2	AlOAl, OAlO, O-H	5.31	29.5	21.6
682.3	5.9	Al-O_{br}, AlOAl, OAlO	0.68	26.5	125.1
754.2	2.2	Al-(OH), AlOAl, AlOH	2.80	247.9	148.5
761.5	2.4	Al-O-H, AlOH	3.68	177.6	175.4
766.2	2.0	Al-O_{br}, Al-O-H, AlOH	1.54	88.8	15.4
778.4	2.0	Al-O-H, O-H, AlOH	1.50	352.3	157.5
794.0	2.9	Al-O-H, AlOH	4.22	56.5	128.1
824.5	1.7	Al-(OH), O-H, AlOH	5.98	64.6	200.0
826.7	1.6	Al-(OH), O-H, AlOH	2.02	115.7	121.0
859.7	1.9	Al-(OH), Al-O-H, AlOH	1.19	69.0	51.8
874.3	1.7	Al-(OH), O-H, AlOH	5.64	71.1	56.7
891.7	2.6	Al-(OH), O-H, AlOH	3.06	269.8	41.1
911.1	2.1	Al-O_{br}, AlOAl, Al-(OH)	1.98	310.5	75.7
1025.7	3.0	Al-O_{br}, O-H, AlOH	1.41	191.6	167.1
1056.1	1.6	Al-O_{br}, Al-(OH), AlOH	2.92	399.3	22.1
3798.7	1.1	O-H	81.66	115.2	1034.8
3816.1	1.1	O-H, AlOH	83.47	7.0	1039.7
3820.2	1.1	O-H	111.15	14.6	1041.2
3824.0	1.1	O-H, AlOH	84.35	6.5	1041.5
3825.5	1.1	O-H, AlOH	85.65	7.0	1042.4
3832.3	1.1	O-H	92.13	6.9	1044.2